(12) INTERNATIONAL APPLICATION PUBLISHED UNDER THE PATENT COOPERATION TREATY (PCT)

(19) World Intellectual Property Organization
International Bureau

(43) International Publication Date
23 July 2009 (23.07.2009)

PCT

(10) International Publication Number
WO 2009/090609 A1

(51) International Patent Classification:
G01N 24/00 (2006.01) *G01R 33/28* (2006.01)
G01R 33/46 (2006.01) *A61B 5/00* (2006.01)

(21) International Application Number:
PCT/IB2009/050144

(22) International Filing Date: 15 January 2009 (15.01.2009)

(25) Filing Language: English

(26) Publication Language: English

(30) Priority Data:
61/022,071 18 January 2008 (18.01.2008) US

(71) Applicant *(for all designated States except US)*: **KONINKLIJKE PHILIPS ELECTRONICS N.V.** [NL/NL]; Groenewoudseweg 1, NL-5621 BA Eindhoven (NL).

(72) Inventors; and

(75) Inventors/Applicants *(for US only)*: **ALBU, Lucian, Remus** [US/US]; c/o PHILIPS IP & S - NL, High Tech Campus 44, NL-5656AE Eindhoven (NL). **MUKHERJEE, Satyen** [US/US]; c/o PHILIPS IP & S - NL, High Tech Campus 44, NL-5656AE Eindhoven (NL).

(74) Agent: **VAN VELZEN, Maaike, M.**; Philips IP & S - Nl, High Tech Campus 44, NL-5656AE Eindhoven, (NL).

(81) Designated States *(unless otherwise indicated, for every kind of national protection available)*: AE, AG, AL, AM, AO, AT, AU, AZ, BA, BB, BG, BH, BR, BW, BY, BZ, CA, CH, CN, CO, CR, CU, CZ, DE, DK, DM, DO, DZ, EC, EE, EG, ES, FI, GB, GD, GE, GH, GM, GT, HN, HR, HU, ID, IL, IN, IS, JP, KE, KG, KM, KN, KP, KR, KZ, LA, LC, LK, LR, LS, LT, LU, LY, MA, MD, ME, MG, MK, MN, MW, MX, MY, MZ, NA, NG, NI, NO, NZ, OM, PG, PH, PL, PT, RO, RS, RU, SC, SD, SE, SG, SK, SL, SM, ST, SV, SY, TJ, TM, TN, TR, TT, TZ, UA, UG, US, UZ, VC, VN, ZA, ZM, ZW.

(84) Designated States *(unless otherwise indicated, for every kind of regional protection available)*: ARIPO (BW, GH, GM, KE, LS, MW, MZ, NA, SD, SL, SZ, TZ, UG, ZM, ZW), Eurasian (AM, AZ, BY, KG, KZ, MD, RU, TJ, TM), European (AT, BE, BG, CH, CY, CZ, DE, DK, EE, ES, FI, FR, GB, GR, HR, HU, IE, IS, IT, LT, LU, LV, MC, MK, MT, NL, NO, PL, PT, RO, SE, SI, SK, TR), OAPI (BF, BJ,

[Continued on next page]

(54) Title: MEASUREMENT METHOD USING NUCLEAR MAGNETIC RESONANCE SPECTROSCOPY AND LIGHT WITH ORBITAL ANGULAR MOMENTUM

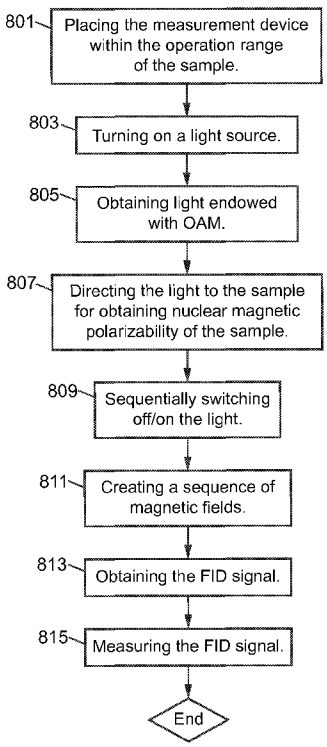

FIG. 8

(57) Abstract: The present invention relates to a non-invasive method of analyzing a fluid sample consisting of molecules, the analysis being based upon nuclear magneticresonance spectroscopy. In the method the following steps are performed: (a) placing (801) an analysis device within anoperation range of the sample to be analyzed; (b) operating (803; 805; 807) in a non-invasive manner the analysis device for obtaining localized nuclear magnetic 5 polarizabilityofthe sample to align nuclei of the molecules to a first direction; (c) relaxing (809) the nuclei to realign them to a second direction and then sequentially (809; 811) aligning and realigning the nuclei to said first and second directions, respectively, for obtaining a free induction decay magnetic signal containing information about the sample; and (d) measuring (815) the obtained free induction decay magneticsignal for analyzing the 10 sample.

WO 2009/090609 A1

CF, CG, CI, CM, GA, GN, GQ, GW, ML, MR, NE, SN, TD, TG).

Declaration under Rule 4.17:

— *as to applicant's entitlement to apply for and be granted a patent (Rule 4.17(ii))*

Published:

— *with international search report*

MEASUREMENT METHOD USING NUCLEAR MAGNETIC RESONANCE SPECTROSCOPY AND LIGHT WITH ORBITAL ANGULAR MOMENTUM

FIELD OF THE INVENTION

The present invention relates to a non-invasive sample analysis method based on nuclear magnetic resonance (NMR) spectroscopy. The invention also relates to a corresponding computer program product, system and device for carrying out the method.

BACKGROUND OF THE INVENTION

NMR is usually pursued in a setup based on a highly homogenous static magnetic field with spatial variation of less than 1ppm, creating nuclear spin precession at a corresponding narrow frequency band of frequencies. However, this setup suffers from the need to employ strong and homogenous magnets, radio frequency (RF) and gradient coils that usually surround the examined sample, such as blood sample or tissue biopsy, and are a major factor in the relative complexity and the high cost of such systems.

NMR has found applications in magnetic nuclear resonance imaging (MRI) (as its sensitivity to the chemical characteristics of tissue components makes it the modality of choice for tissue characterization and differentiating soft tissues), fluid chemical analysis of small molecules and biomolecules (protein-ligand interactions, protein folding, protein structure validation, protein structure determination), solid state analysis (structural), dynamics of time-variable systems (functional MRI), etc.

A company called "TopSpin Medical" has recently revealed an intra venous magnetic nuclear resonance imaging (IVMRI) catheter with a static magnetic field of about 0.2 Tesla generated by strong permanent magnets located at the tip of a catheter. This company has developed a self contained "inside-out" miniature MRI probe in a tip of an intravascular catheter that allows for local high-resolution imaging of blood vessels without the need for external magnets or coils. This probe is shown in Figure 1. The advantages of this technique range from the very practical aspect of a low-cost system, since no expensive external setup is required, accessibility to the patient during the procedure, compatibility with existing interventional tools and finally resolution and diffusion contrast capabilities that are unattainable by conventional clinical MRI, due to the strong local gradients created by the probe and its proximity to the examined tissue. This intravascular probe serves as a first example for a wide range of applications for this method, which in the near future may revolutionize the field of clinical MRI. The medical applications for this technology include

for instance detection and staging of prostate cancer, imaging tumors in the colon, lung and breast and intravascular imaging of the peripheral vasculature.

Micro NMR coils are also known for a skilled man in the art. Developments of these "micro MRI" devices depend on the existence of high quality receiving coils. Microelectromechanical systems (MEMS) breakthroughs have made possible this new technology for the micro fabrication of Helmholtz micro coils for NMR spectroscopy. These Helmholtz micro coils demonstrate superior NMR performance in terms of spin excitation uniformity compared to planar micro coils. The improved spin excitation uniformity opens the way to advanced chemical analysis by using complex RF-pulse sequences. The fabricated Helmholtz coils have Q-factor greater than 20 due to electroplated coil turns and vias, which connect the lower and upper turns. For analyzing living cells, mechanical filters can be integrated for sample concentration and enhanced detection.

It has further been developed a non-invasive blood analysis method based on combined imaging and confocal Raman spectroscopy. With this technology, in-vivo Raman spectra can be obtained that resemble in-vitro spectra with respect to shape and intensity.

The ingenious apparatus developed within the context is capable of detecting the position of a shallow, i.e. roughly 1mm under the skin, blood vessel with a 25 m resolution, and then precisely collect the backscattered light with a confocal microscope (25 m resolution depth of focus). Unfortunately the poor Raman response and closeness of the water and glucose spectral specificity make this non-invasive blood analysis procedure too expensive for the time being.

NMR requires orienting a part of the nuclei magneton (spins) population along a chosen spatial direction. When oriented, the population is in a polarized state. This is usually achieved with strong magnetic fields, which are not attenuated by diamagnetic materials (biological tissue, fluids etc.). The net polarization achieved using magnetic fields is usually on the order of 5 to 25 parts per million. The nuclei spins of a material can be locally oriented by radiating the sample with circularly polarized light. Methods using circularly polarized light are able to achieve high levels of polarization, up to 40%, under the right circumstances. Polarizations in this order of magnitude are considered hyperpolarized. Hyperpolarizability is obtained through the hyperfine spin-spin interaction electron-nucleus, the electron-photon spin exchange and the electronic-spin population saturation due to Fermi's exclusion principle applied to molecule's electrons.

Optical pumping is used to produce hyperpolarized gases. Hyperpolarized gases have found a steadily increasing range of applications in MRI and NMR. They can be considered as a new class of MR contrast agent or as a way of greatly enhancing the temporal resolution of the measurement of processes relevant to areas as diverse as materials science

and biomedicine. The physics of producing hyperpolarization involves irradiating samples of Na with intense circularly polarized lasers of a wave length corresponding to one of the absorption bands for Na, followed by a "mechanical" polarization transfer to inert ^{129}Xe. The last is used as contrast agents in MRI and polarization transfer for other nuclear species for low-field imaging.

The NMR effect can be observed and measured with optical methods. All Optical NMR hyperfine interactions allow for flip-flop spin scattering. This means that an electron can flip its spin by flipping simultaneously a nucleus into the other direction. This leads to a dynamic polarization of the nuclear spins. If the electron spin levels are saturated by a driving field, i.e. the population of the upper spin state is made equal to that of the lower state, such flip-flop processes try to re-establish thermal equilibrium, resulting in a nuclear spin polarization, which is described by a Boltzmann factor where the electron Zeeman splitting enters. Because the electron splitting is usually 1000 times larger than the nuclear splitting, the nuclei end up in an up to 1000 times enhanced polarization compared to their thermal equilibrium value – also known as an Overhauser effect.

Yet, another application of light angular momentum with magnetons is a high sensitivity-high frequency magnetometer. This solves one of the challenges raised by observing NMR effects, which is being able to measure the transient response of the magnetic fields produced by spinning nuclei. A magnetometer has been demonstrated operating by detecting optical rotation due to the precession of an aligned ground state in the presence of a small oscillating magnetic field. The projected sensitivity is around 20pG/pHz (RMS).

In 1992 Allen et al., "Optical angular momentum", ISBN 0 7503 0901 6, verified the existence of light endowed with orbital angular momentum (OAM). Theoretical understanding and experimental evidence lead to applications, where light with OAM interacts with matter: optical tweezers, high throughput optical communication channels, optical encryption technique, optical cooling (Bose-Einstein condensates), entanglement of photons with OAM, entanglement of molecule quantum numbers with interacting photons OAM.

The Micro NMR is an appealing chemical analysis device for being included in an ePill device or in an inexpensive non-invasive blood analysis apparatus. It shall consume low power, be confined within a small volume and shall not include any paramagnetic materials (FDA). "TopSpin Medical" micro NMR or other "fixed magnet based" NMR are not suitable for the purpose, since these include a permanent magnet, require long acquisition time and hence consume power. An ePill is a small electronic device that is swallowed by a patient for performing an analysis of internal organs of the patient.

Photon-electron spin interaction has been extensively observed and modeled and it is the basis of the optical pumping technology for hyperpolarizability of gases. Unfortunately, this technique is not capable for producing fluid hyperpolarizability, due to thermal molecular movement and interactions.

Photon OAM interactions with nuclei has been recently analyzed as a method of controlling the spin-spin interaction within nuclei. It uses energetic X rays, not desirable for "in-vivo" applications.

Furthermore, by applying a constant magnetic field to a sample containing N nuclei, at room temperature, one can calculate the maximum number of oriented nuclei (Boltzmann distribution), which is around $10^{-5}N$. In order to extract a significant magnetic signal from the sample, one has to implement high quality factor coils or enlarge the size of the sample. In both cases the volume occupied by the receiver shall increase, which makes the permanent magnet micro NMR difficult to integrate within an ePill.

Thus, the object of the present invention is to provide an improved method and apparatus for sample analysis based on NMR spectroscopy.

SUMMARY OF THE INVENTION

According to a first aspect of the invention there is provided a non-invasive method of analyzing a fluid sample consisting of molecules, the analysis being based upon nuclear magnetic resonance spectroscopy, the method comprising the following steps:

- placing an analysis device within an operation range of the sample to be analyzed;
- operating in a non-invasive manner the analysis device for obtaining localized nuclear magnetic polarizability of the sample to align nuclei of the molecules to a first direction;
- relaxing the nuclei to realign them to a second direction and then sequentially aligning and realigning the nuclei to said first and second directions, respectively, for obtaining a free induction decay magnetic signal containing information about the sample; and
- measuring the obtained free induction decay magnetic signal for analyzing the sample.

This provides clear advantages, namely for instance the nuclear magnetic polarizability is obtained in a well defined, localized space. Furthermore, if the polarizability is obtained by using light endowed with OAM, there is no need to use strong magnets for obtaining the nuclear magnetic polarizability. If these magnets are applied, the whole body of the patient will become polarized. This is clearly undesirable, since in that case it would be

difficult to obtain correct measurement results from a desired location from the body. The reason for this is that the measurement signals form all over the body would interfere with the desired measurement signal.

Moreover, in case strong magnets are used for obtaining the polarizability, it is important that the magnetic field is uniform. In the present invention, this is not an issue, since no magnets are used for this purpose. Also, in the present invention there is no need to place coils all over the body for measuring the free induction decay (FID) signal, only two coils placed in close proximity suffice for obtaining the FID signal.

A further advantage when the light with OAM is employed is that the FID signal is much stronger than the corresponding signal obtained by using traditional NMR spectroscopy methods. Thus, the sensitivity of the measurement technique is greatly improved. The obtained FID signal is also less noisy and better resolution can be achieved. As a consequence smaller samples can be analyzed.

According to a second aspect of the invention there is provided a computer program product comprising instructions for implementing the method according the first aspect of the invention when loaded and run on computer means of a sample analysis device.

According to a third aspect of the invention there is provided a fluid analysis device for analyzing a fluid sample non-invasive analysis device for analyzing a fluid sample consisting of molecules, the analysis being based upon nuclear magnetic resonance spectroscopy, the device comprises:

- means for obtaining in a localized space nuclear magnetic polarizability of the sample to align magnetons of the molecules to a first direction;
- means for relaxing the magnetons to realign them to a second direction;
- means for sequentially aligning and realigning the magnetons to said first and second directions, respectively, for obtaining a free induction decay magnetic signal containing information about the sample; and

means for measuring the obtained free induction decay magnetic signal for analyzing the sample.

According to a fourth aspect of the invention there is provided a measurement system comprising the analysis device in accordance with the third aspect, wherein the measurement system further comprises:

- a light source for creating light;
- means for introducing orbital angular momentum into the light;
- means for obtaining a focused light beam; and

- means for illuminating the sample with the focused light beam carrying orbital angular momentum for obtaining nuclear magnetic polarizability of the sample.

BRIEF DESCRIPTION OF THE DRAWINGS

Other features and advantages of the invention will become apparent from the following description of non-limiting exemplary embodiments, with reference to the appended drawings, in which:

- Figure 1 shows a side view of a medical IVMRI probe;
- Figure 2 is a graph showing a potential vector f as a function of a radial coordinate ρ;
- Figure 3 is a graph showing the potential vector f as a function of the radial coordinate ρ by using other parameters as those used for Figure 2;
- Figure 4 shows possible OAM-molecule interactions;
- Figure 5 is a block diagram of an analysis system for carrying out the fluid analysis in accordance with an embodiment of the present invention;
- Figure 6 shows a structural view of a processing unit of a CMOS MEMS device;
- Figure 7 is a schematic illustration of a CMOS MEMS analysis device in accordance with an embodiment the present invention;
- Figure 8 is a flow chart depicting a method of performing a high resolution fluid analysis in accordance with an embodiment of the present invention;

DETAILED DESCRIPTION OF THE INVENTION

In the following description a non-limiting exemplary embodiment of the invention for carrying out high resolution sample analysis will be described in more detail. Also the corresponding measueremnt system will be described by use of exemplary block diagrams. In this exemplary embodiment the nuclear magnetic polarizability of the sample is obtained by applying light endowed with OAM to the sample. It is to be noted that other suitable methods, current or future, may be envisaged for obtaining the nuclear magnetic polarizability. One currently available method includes the use of high energy x-rays. However, this method has the drawback that these rays have a destructive effect on a human body. Thus, the light endowed with OAM is preferred and an embodiment based on the light with OAM is explained next in more detail. Furthermore, in the following example, the sample to be measured is blood in a blood vessel of a human body.

The OAM of absorbed photons is transferred to interacting molecules (angular momentum conservation) and as a consequence:

- Electron state reaches a saturated spin state;

- Angular momentum of the molecule (around centre of mass of the molecule) is increased and oriented along the propagation axis of incident light; and
- All magnetic magnetons precession movement associated with the molecules (including electrons and nucleons) are oriented along the propagation axis of incident light.

The above make possible to obtain nuclear magnetic polarizability of fluids by illuminating them with light carrying OAM and possibly spin, i.e. angular momentum, and implement an NMR device without a permanent magnet. For instance hyperpolarizability of blood within shallow capillarity (< 1mm deep) can be obtained with regular NMR coils and techniques to detect the metabolites NMR spectrum lines and produce a quantitative report on the concentration of metabolites in the blood. As an example, the blood glucose concentration can be simply detected.

The quantum electrodynamics (QED) framework can be considered as a starting point for explaining the interaction of photons with OAM with matter. This has been applied for a hydrogenic model, and it has been found out that the OAM part of the incident light induces a rotation of the molecule, of a momentum equal to the light's momentum. This finding has been confirmed by stating from a more general Bessel model of light with OAM.

The spontaneous or stimulated emission of photons endowed with OAM are phenomena not yet understood, modeled or experimentally proven. Therefore, the generation of beams with OAM is accomplished through optical means of spatial phase change, interference and diffraction of Gaussian beams. Four methods (five if the two methods using cylindrical lenses are considered separate methods) are available as summarized in Table 1. In the table the power conversion efficiency is the ratio of the output power (beam with OAM) to the power of the input beam. Currently the highest OAM number obtained in a laboratory is as high as 10000 $\hbar$ L per photon. This is obtained by an elliptical Gaussian beam focused by a cylindrical lens.

Table 1: Methods for generating light with OAM.

Input beam type	*Mode Converter*	*OAM Variability*	*Power Conversion Efficiency*	*Notes*
Hermite Gauss $TEM_{m,n}$ laser	Cylindrical lenses	NO	~95%	Modified laser cavities and out of cavity cylindrical lenses to convert usual Hermite-Gauss $TEM_{m,n}$ laser modes into Laguerre-Gauss modes. The orbital angular momentum number l is given by $l = m - n$, so that high-order HG modes must be generated first.
Gauss TEM_{00} laser	Cylindrical lenses posed at different angles	YES	~95%	A set of cylindrical lenses posed at different angles in the path of a TEM_{00} laser beam can produce a beam carrying orbital angular momentum (not eigenstate!). Beams carrying up to $10000\hbar$ angular momentum per photon have been produced in this way.
Gauss TEM_{00} laser	Phase plate	NO	10..80%	Transparent plate micro machined such that the OAM phase singularities are mapped to the geometry of the plate.
Gauss TEM_{00} laser	Hologram plate	NO	NA	Holographic plate that maps the OAM phase singularities to the holographic pattern on the plate.

Gauss TEM_{00} laser modes	Computer generated hologram with space light modulator	YES	~2%	Computer generated holograms that map the OAM phase singularities to holographic patterns. The holograms are applied to Space Light Modulator devices illuminated with lasers; may convert TEM_{00} laser beams into $LG_{m,n}$ beams.

Looking at the interaction of light endowed with OAM with molecules, it has been found that an exchange of orbital angular momentum in an electric dipole transition occurs only between the light and the centre of mass motion. In other words internal ''electronic-type'' motion does not participate in any exchange of orbital angular momentum in a dipole transition. It has been proved that the rotation/vibration of irradiated molecules increases with the value of the OAM. It has been further shown that photon OAM interacts with nucleons magnetons. Such transitions require photons with a high angular momentum and could be used for fine-tuning the processes of nuclear multipolarity transitions.

The NMR analysis technique lies on the following steps:

1. The sample nuclear magnetic momenta are oriented (precession movement) along a selected spatial direction. This is usually achieved with a strong magnetic field or – within more recent applications – with polarized light.
2. While in nuclear polarized state, one applies to the sample a sequence of magnetic fields, which triggers the free induction decay (FID) magnetic signal, representing the magnetic nuclei relaxation time from the magnetic sequence state to the polarized state.
3. The parameters in a nuclear magnetic resonance (NMR) FID signal contain information that is useful in biological and biomedical applications and research.

In contrast to the constant magnetic field NMR, the optical pump can achieve about 100% hyperpolarizability of the sample, i.e. about N nuclei will have the precession of their magnetic momentum oriented along the direction of propagation of pumping light. This makes possible the reduction of the sample and receiving coils, therefore the device could be integrated within an ePill. The signal to noise ratio is therefore improved by optical pumping as well as the power budget for the low noise amplifier (LNA) coil receiver.

The nuclear magnetic polarizability in this embodiment relies on a new method to orient the nuclei of a sample along a selected spatial direction using the interaction of light with OAM with molecules. The following sections focus on the theoretical explanation of this interaction and an experimental proof of the concept.

Following notations and symbols are used throughout the remaining description:

$\Re(z), \Im(z), \|z\|$	real part, imaginary part and modulus of a complex number z
$\vec{1}_x, \vec{1}_y, \vec{1}_z$ *or* $\hat{x}, \hat{y}, \hat{z}$	linear independent unit vectors for Cartesian coordinates system $(Oxyz)$
$\vec{1}_\rho, \vec{1}_\theta, \vec{1}_z$ *or* $\hat{\rho}, \hat{\theta}, \hat{z}$	linear independent unit vectors for Cartesian coordinates system $(O\rho\theta z)$
$\vec{v}_m, v_{m,\vec{\theta}}, v_{m,\vec{\rho}}, v_{m,\vec{z}},$	indexed *m* vector with its linear components in a cylindrical coordinates system: $\vec{v}_m = v_{m,\vec{\rho}}\,\vec{1}_\rho + v_{m,\vec{\theta}}\,\vec{1}_\theta + v_{m,\vec{z}}\,\vec{1}_z$
$\vec{r}$	$x\vec{1}_x + y\vec{1}_y + z\vec{1}_z$
c	speed of light in vacuum
$h\,(\hbar)$	Plank constant $(h/2\pi)$
$\vec{A}(\vec{r},t)$	electromagnetic potential vector
$\vec{A}_{pol}$	electromagnetic potential vector polarization
$\vec{E}(\vec{r},t)$	electric intensity vector field
$\vec{B}(\vec{r},t)$	magnetic intensity vector field
v	frequency
λ	wavelength (c/v)
ω	angular frequency $2\pi\lambda$
$\vec{k}$	wave vector $2\pi/\lambda\,\vec{1}_z$, $k = \|\vec{k}\| = 2\pi/\lambda$
i	complex unit $\sqrt{-1}$
w_o	beam radius (waist) at $z = 0$

z_R	Raileight range, distance z at which beam section area doubles
$w(z)$	beam radius $\sqrt{1+(z/z_R)^2}$
$L_n^k(x)$	n^{th} order generalized Laguerre polynominal with parameter k evaluated at x, $L_n^k(x)=\sum_{m=0}^{n}(-1)^m\frac{(n+k)!}{(n-m)!(k+m)!m!}x^m.\forall k\in\mathbb{N},\forall x\in\mathbb{R},L_0^k(x)\equiv 1$
$\vec{v}_{l,p}$	vector associated to a Laguerre-Gauss electromagnetic wave of order l and parameter p.
$\mu_n=\frac{e_n\hbar}{2m_nc}$	*Bohr magneton* for a particle with charge m_n

Electromagnetic equations for Laguerre-Gauss beams

The classic electromagnetic wave equation for the potential vector $\vec{A}(\vec{r},t)$ (derived from Maxwell's equations) is:

$$\nabla^2\vec{A}(\vec{r},t)-\frac{1}{c^2}\frac{\partial^2\vec{A}(\vec{r},t)}{\partial t^2}=0 \qquad (1:1)$$

with $\nabla\cdot\vec{A}=0$. Assuming a null charge distribution in space $\phi(\vec{r},t)=0$, the corresponding electromagnetic field strengths are:

$$\begin{aligned}\vec{E}(\vec{r},t)&=-\nabla\phi-\frac{\partial}{\partial t}\vec{A}(\vec{r},t)=-\frac{\partial}{\partial t}\vec{A}(\vec{r},t)\\ \vec{B}(\vec{r},t)&=\nabla\times\vec{A}(\vec{r},t)\end{aligned} \qquad (1:2)$$

Let us look for a solution of the wave equation propagating along $\overrightarrow{Oz}$ axis of the form:

$$\vec{A}(\vec{r},t)=\vec{A}_{pol}u(\vec{r})e^{i(\vec{k}\cdot\vec{z}-\omega t)} \qquad (1:3)$$

Replacing in (1:1) and assuming $\vec{A}_{pol}$ independent of space and time, we obtain the equation for the spatial distribution $u(\vec{r})$:

$$\frac{\partial^2u(\vec{r})}{\partial x^2}+\frac{\partial^2u(\vec{r})}{\partial y^2}+2ik\frac{\partial u(\vec{r})}{\partial z}=0 \qquad (1:4)$$

Spatial symmetry within the paraxial approximation for Gaussian beams pleads for cylindrical coordinates $u(\vec{r}) = u(\rho,\theta,z)$. For Laguerre-Gauss beams, the solution of (1:4) is:

$$u_{l,p}^{LG}(\rho,\theta,z) = \frac{C_{l,p}}{w(z)} R^{|l|} e^{-\left(\frac{R}{\sqrt{2}}\right)^2} L_p^{|l|}\left(R^2\right) e^{-i\left(\frac{kz}{4}\left(\frac{Rw_0}{z_R}\right)^2 + l\theta - (2p+l+1)\arctan\left(\frac{z}{z_R}\right)\right)} \quad (1:5)$$

with: $C_{l,p} = \frac{1}{2^{\frac{|l|}{2}} L_p^{|l|}(0)}$ a normalization constant and $R = R(z) = \frac{\sqrt{2}\rho}{w(z)}$.

For a well-collimated beam (collimation sustained for long distances), one might assume $z_R >> z$. Taking (1:5) at the limit for $z_R \to \infty$ we find:

$$u_{l,p}^{LG}(\rho,\theta,z) = \frac{C_{l,p}}{w_0} R^{|l|} e^{-\left(\frac{R}{\sqrt{2}}\right)^2} L_p^{|l|}\left(R^2\right) e^{-il\varphi} \quad (1:6)$$

The wave equation solution for the potential vector, in cylindrical coordinates, paraxial approximation, Laguerre-Gauss isomorphic is:

$$A(\vec{r},t) = \vec{A}_{pol} u_{l,p}^{LG}(\rho,\theta,z) e^{i(\vec{k}\cdot\vec{z}-\omega t)} = \vec{A}_{pol} \frac{C_{l,p}}{w_0} R^{|l|} e^{-\left(\frac{R}{\sqrt{2}}\right)^2} L_p^{|l|}\left(R^2\right) e^{i(kz-\omega t-l\theta)} \quad (1:7)$$

The potential vector is a function of the radial coordinate ρ through the function:

$$f(R) = f_{l,p}(\rho) = \frac{C_{l,p}}{w_0} R^{|l|} e^{-\left(\frac{R}{\sqrt{2}}\right)^2} L_p^{|l|}\left(R^2\right), \text{ with } R = R(0) = \frac{\sqrt{2}\rho}{w_0} \quad (1:8)$$

A remarkable and useful solution is the case $p = 0$:

$$f_{l,0}(\rho) = \frac{1}{w_0}\left(\frac{R}{\sqrt{2}}\right)^{|l|} e^{-\left(\frac{R}{\sqrt{2}}\right)^2} = \frac{1}{w_0}\left(\frac{\rho}{w_0}\right)^{|l|} e^{-\left(\frac{\rho}{w_0}\right)^2} \quad (1:9)$$

$f_{l,0}(\rho)$ is 0 for $\rho \in \{0,\infty\}$, has only one maxima for $R_{\max} = \frac{\sqrt{2}\rho_{\max}}{w_0} = \sqrt{|l|}$, and the value at any point is proportional to $1/w_0$. This function does not depend on any physical parameters of the electromagnetic wave (other than w_0, and l). Figure 2 gives the plot for $f(R) = f_{l,0}(\rho)$. In this figure $R \in [0,6]$, $l \in \{0,6\}$ and w_0=1. An increase of l leads to an increase of the beam waist with $\sqrt{|l|}$.

The angular momentum associated to the Laguerre-Gauss beams is $L_z = \left\| \vec{r} \times \vec{S} \right\| = l\hbar$.

If l is kept constant and p increases as a positive real number, the function $f_{l,p}(\rho)$ has an increasing number of local extreme points. Figure 3 plots a family of curves with $l = 1, p \in \{0,..,5\}, w_0 = 1$. For this graph, the function $f_{l,p}(\rho)$ has been normalized to $\sqrt{\int_0^\infty f_{l,p}^2(\rho) d\rho}$. It is interesting to note that the gradient increases towards the origin for large p's as well as that the distance between peaks decreases. This marks a change in the sense of the fields for consecutive peaks as well as a higher field gradient for small R's.

From equations (1:2) and (1:7) we can extract the electric and magnetic field strengths:

$$\vec{E}(\vec{r},t) = \vec{E}_{l,p}(\vec{r},t) = \vec{E}_{pol}(\omega) f_{l,p}(\rho) e^{i(kz-\omega t-l\theta)} \qquad (1:10)$$

where: $\vec{E}_{pol}(\omega) = -i\omega \vec{A}_{pol}$. For propagation in isotropic linear media, the electric field strength is a vector parallel to $\vec{A}_{pol}$. This is not the case with the magnetic strength field. Let us choose $\vec{A}_{pol}$ parallel to $\vec{1}_x$. In cylindrical coordinates we obtain:

$$\vec{A}_{pol} = A_{pol}\vec{1}_x = A_{pol,\vec{\rho}}\vec{1}_\rho \qquad (1:11)$$

with: $A_{pol,\vec{\rho}} = A_{pol}$ and $A_{pol,\vec{\theta}} = A_{pol,\vec{z}} = 0$. The gradient operator in cylindrical coordinates is:

$$\nabla = \frac{\partial}{\partial\rho}\vec{1}_\rho + \frac{1}{\rho}\frac{\partial}{\partial\theta}\vec{1}_\theta + \frac{\partial}{\partial z}\vec{1}_z \qquad (1:12)$$

The magnetic field is:

$$\vec{B}(\vec{r},t) = -\frac{\partial A_{\vec{\rho}}}{\partial z}\vec{1}_\theta - \frac{1}{\rho}\frac{\partial A_{\vec{\rho}}}{\partial\theta}\vec{1}_z \qquad (1:13)$$

with $A_{\vec{\rho}} = A_{pol,\vec{\rho}} f_{l,p}(\rho) e^{i(kz-\omega t-l\theta)}$. Calculations lead to:

$$\vec{B}(\vec{r},t) = \vec{B}_{l,p}(\vec{r},t) = iA_{pol,\vec{\rho}} f_{l,p}(\rho) e^{i(kz-\omega t-l\varphi)}\left(-k\vec{1}_\theta + \frac{l}{\rho}\vec{1}_z\right) \qquad (1:14)$$

This relation shows that the magnetic field strength has components not only in $\vec{1}_\theta$ direction, but also in $\vec{1}_z$ direction. The amplitude of the latest direction is proportional to l and decays with the distance from the origin.

The Poynting vector is a classical measure of the energy flux carried by the electromagnetic wave:

$$\vec{S}(\vec{r},t) = \vec{E}(\vec{r},t) \times \vec{B}(\vec{r},t) \qquad (1:15)$$

Looking at the decomposition from (1:3) and (1:12) we obtain:

$$\frac{\vec{S}(\vec{r},t)}{-i\omega} = A_{\vec{\rho}}\vec{\mathbf{1}}_{\rho} \times \left(\frac{\partial A_{\vec{\rho}}}{\partial z}\vec{\mathbf{1}}_{\theta} + \frac{1}{\rho}\frac{\partial A_{\vec{\rho}}}{\partial \theta}\vec{\mathbf{1}}_{z} \right) \qquad (1:16)$$

The cylindrical coordinates satisfy $\vec{\mathbf{1}}_{\rho} \times \vec{\mathbf{1}}_{\theta} = \vec{\mathbf{1}}_{z}, \vec{\mathbf{1}}_{z} \times \vec{\mathbf{1}}_{\rho} = \vec{\mathbf{1}}_{\theta}, \vec{\mathbf{1}}_{\theta} \times \vec{\mathbf{1}}_{z} = \vec{\mathbf{1}}_{\rho}$, and the previous expression for $\vec{S}(\vec{r},t)$ is:

$$\frac{\vec{S}(\vec{r},t)}{-i\omega} = A_{\vec{\rho}}\frac{1}{\rho}\frac{\partial A_{\vec{\rho}}}{\partial \theta}\vec{\mathbf{1}}_{\theta} + A_{\vec{\rho}}\frac{\partial A_{\vec{\rho}}}{\partial z}\vec{\mathbf{1}}_{z} \qquad (1:17)$$

This shows that there is a flow of electromagnetic energy with two components:

- $\vec{\mathbf{1}}_{z}$ direction component, proportional to the spatial derivative of the potential vector along the beam propagation (as for a plane wave); and
- $\vec{\mathbf{1}}_{\theta}$ direction component, about the axis of the beam propagation. This component is proportional to the angular change of the potential vector around the beam propagation: the Poynting vector rotates about the beam propagation axis.

Let us replace the value of $A_{\vec{\rho}}$ in the last equation:

$$\vec{S}(\vec{r},t) = \vec{S}_{l,p}(\vec{r},t) = \omega A_{\vec{\rho}}^{2}\left(-\frac{l}{\rho}\vec{\mathbf{1}}_{\theta} + k\vec{\mathbf{1}}_{z} \right) \qquad (1:18)$$

This relation shows that the rotational energy flow is proportional to *l*. It is interesting to find the ratio of those two components:

$$s_{l,p}^{\theta z}(\vec{r},t) = \frac{\vec{S}_{l,p}(\vec{r},t)\cdot\vec{\mathbf{1}}_{\theta}}{\vec{S}_{l,p}(\vec{r},t)\cdot\vec{\mathbf{1}}_{z}} = -\frac{l}{k\rho} = -\frac{1}{R}\frac{\lambda}{w_0}\frac{l}{\sqrt{2}\pi} \qquad (1:19)$$

The ratio $s_{l,p}^{\theta z}(\vec{r},t)$ is time independent. It is also linear with *l*, therefore the electromagnetic energy flow about the beam propagation axis increases proportional to *l*. The rotational energy transferred to molecules interacting with light is increased with *l*. This holds if λ/w_0 is kept constant for different *l*'s. The magnitude of $s_{l,p}^{\theta z}(\vec{r},t)$ reaches higher values for small w_0, which makes the observation of the mentioned dependence easier for tightly focused beams.

Theory: Photon OAM interactions with molecules

The manifestation of OAM in the interactions of twisted beams with matter has been explored theoretically, leading to predictions that a light-induced torque can be used to control the rotational motion of atoms. It has been shown that OAM is an intrinsic property

of all types of azimuthal phase-bearing light, independent of the choice of axis about which the OAM is defined. The engagement of twisted beam OAM can be classified in terms of intrinsic and extrinsic interactions, i.e. those relating to electronic transitions, and those concerned with centre of mass motion.

On such grounds it might be argued that, in its interaction with an electronically distinct and isolated system such as a free atom or a molecule, intrinsic OAM should manifest through an exchange of orbital angular momentum between the light and matter, just as photon spin angular momentum manifests itself in the selection rules associated with the interactions of circularly polarized light.

It has been further shown that the internal electronic-type motion does not exchange any OAM with the light beam in this leading order of multipole coupling. On detailed analysis, it transpires that only in the weaker electric quadrupole interaction, or in yet higher order multipoles, is there an exchange involving all three subsystems, namely the light, the atomic centre of mass and the internal motion. In the electric quadrupole case, one unit of orbital angular momentum is exchanged between the light beam and the internal motion, resulting in the light beam acquiring of $(l\pm1)$. OAM, which are then transferred to the centre of mass motion.

Theory: QED transition matrix for OAM beams

Let us consider a molecule made out of n_{mol} particles, with masses m_n, charges e_n, linear momentum $\vec{p}_n$, spin $\vec{s}_n$, $n \in \{1,..,n_{mol}\}$, n_e electrons and n_{mol} - n_e nucleons.

The molecule interacts with a light beam propagating along Oz axis, with energy $\hbar\omega$, linear momentum $\hbar\vec{k}$ and orbital angular momentum of $\hbar l$. The reference frame origin is chosen at the beam waist of the light beam, as described above.

We will express the transition rate of the molecule from initial state $|i\rangle$ to final state $|f\rangle$, emphasizing the contribution of the orbital angular momentum to this transition. According to Fermi's golden rule, the transition rate W_{fi} (transitions per seconds per molecule) is:

$$W_{fi} = \frac{dP_{fi}}{dt} = h\left|V_{fi}\right|^2 D\left(E_{fi}\right) = h\left|\left\langle f\left|H_{fi}^{(1)}\right|i\right\rangle\right|^2 D\left(E_{fi}\right) \qquad (3:1)$$

P_{fi} is the probability of the transition from state $|i\rangle$ (energy E_i) to state $|f\rangle$ (energy E_f) under an electromagnetic excitation defined by the perturbation potential (Hamiltonian) $H_{fi}^{(1)}$ and density of states of $D(E_{fi})$ (where $E_{fi} = E_f - E_i$).

Let us express the matrix element for the transition $M_{fi} = \langle f | H_{fi}^{(1)} | i \rangle$. The Hamiltonian of the molecule-light system is:

$$H(t) = \sum_{n=1}^{n_{mol}} \left[\frac{1}{2m_n} \left(\vec{p}_n - \frac{e_n}{c} \vec{A}(\vec{r}_n, t) \right) \bullet \left(\vec{p}_n - \frac{e_n}{c} \vec{A}(\vec{r}_n, t) \right) - \frac{e_n \hbar}{2m_n c} \left(\vec{s}_n \bullet \nabla_n \times \vec{A}(\vec{r}_n, t) \right) \right] + V_{NN} + V_{NE} + V_{EE} \quad (3:2)$$

with:

V_{NN}: Total interaction energy for nucleons;

V_{NE}: Total electron-nucleon interaction energy; and

V_{EE}: Total interaction energy for electrons.

The "not-perturbed" Hamiltonian includes only terms of the above, which do not depend on the light beam, independent of $\vec{A}(\vec{r}_n, t)$. The expression $H_n(t)$ shown in equation (3:3), describes the energetic interaction of light with each particle that composes the molecule. The Hamiltonian for a particle *n* interacting with light is:

$$\begin{aligned} H_n(t) &= \frac{1}{2m_n} \left(\vec{p}_n - \frac{e_n}{c} \vec{A}(\vec{r}_n, t) \right) \bullet \left(\vec{p}_n - \frac{e_n}{c} \vec{A}(\vec{r}_n, t) \right) - \frac{e_n \hbar}{2m_n c} \left(\vec{s}_n \bullet \nabla_n \times \vec{A}(\vec{r}_n, t) \right) = \\ &= \frac{1}{2m_n} \left(\vec{p}_n \bullet \vec{p}_n - \frac{e_n}{c} \left(\vec{A}(\vec{r}_n, t) \bullet \vec{p}_n + \vec{p}_n \bullet \vec{A}(\vec{r}_n, t) \right) + \left(\frac{e_n}{c} \right)^2 \vec{A}(\vec{r}_n, t) \bullet \vec{A}(\vec{r}_n, t) \right) \\ &\quad - \frac{e_n \hbar}{2m_n c} \left(\vec{s}_n \bullet \nabla_n \times \vec{A}(\vec{r}_n, t) \right) \end{aligned} \quad (3:3)$$

Because of the QED rule that the potential acts only once, the term $\vec{A}(\vec{r}_n, t) \bullet \vec{A}(\vec{r}_n, t)$ does not enter this problem. With $\mu_n = \frac{e_n \hbar}{2m_n c}$ (for an electron, μ_n represents the "Bohr magneton") and replacing the linear momentum vector with its quantum operator $\vec{p}_n \to i\hbar\nabla_n$, the Hamiltonian turns into:

$$\hat{H}_n(t) = \underbrace{-\frac{\hbar^2}{2m_n} |\nabla_n|^2}_{\hat{H}_n^{(0)}} \underbrace{-i\mu_n \left[\vec{A}(\vec{r}_n, t) \bullet \nabla_n + \nabla_n \bullet \vec{A}(\vec{r}_n, t) + \vec{s}_n \bullet \nabla_n \times \vec{A}(\vec{r}_n, t) \right]}_{\hat{H}_{int,n}(t) = \hat{H}_n^{(1)}} \quad (3:4)$$

The $^{(0)}$ index marks the time independent Hamiltonian, while the $^{(1)}$ index represents the light-molecule interaction Hamiltonian (perturbation).

$$\hat{H}^{(0)} = V_{NN} + V_{EE} + V_{NE} + \sum_{n=0}^{n_{mol}} \hat{H}_n^{(0)}$$
$$\hat{H}^{(1)} = \hat{H}^{(1)}(t) = \sum_{n=0}^{n_{mol}} \hat{H}_n^{(1)} \qquad (3:5)$$

The time dependent Schrödinger equation is:

$$i\hbar \frac{\partial}{\partial t}\Psi(\vec{r},t) = \left[H^{(0)} + H^{(1)}(t)\right]\Psi(\vec{r},t) \qquad (3:6)$$

With the stationary states eigenfunctions ψ_k and eigenvalues E_k satisfying:

$$H^{(0)}\psi_k = E_k\psi_k \ , k \in \{1,..,N\} \qquad (3:7)$$

And a general solution of

$$\Psi(\vec{r},t) = \sum_k c_k(t)\psi_k(\vec{r})e^{-\frac{i}{\hbar}E_k t} \qquad (3:8)$$

The first order perturbation theory gives:

$$\frac{dc_b(t)}{dt} = \frac{1}{i\hbar}\sum_{k=0}^{N} H_{b\leftarrow k}^{(1)}(t)c_k(t)e^{i\omega_{bk}t} \qquad (3:9)$$

with: $H_{b\leftarrow k}^{(1)}(t) = \langle_b | H_{bk}^{(1)}(t) |_k \rangle$ and $\omega_{bk} = (E_b - E_k)/\hbar$. Initial conditions assume that before the interaction the molecule is in state $\Psi(\vec{r}, t \le 0) = \psi_a \left(c_a^{(0)} = 1\right)$ and the final state ψ_b is not occupied $\left(c_b^{(0)} = 0\right)$. Replacing those in (3:9) we obtain $c_k(t \le 0) = c_k^{(0)} = \delta_{ka}$, ($\delta_{ka}$: Kronecker symbol) and

$$\frac{dc_b(t)}{dt} = \frac{1}{i\hbar}H_{b\leftarrow a}^{(1)}(t)\delta_{ka}e^{i\omega_{ba}t} \Leftrightarrow c_b(t) = \frac{1}{i\hbar}\int_0^t H_{b\leftarrow a}^{(1)}(\tau)e^{i\omega_{ba}\tau}\,d\tau - c_b^{(0)} \qquad (3:10)$$

We will express the time dependent perturbation $H_{b\leftarrow a}^{(1)}(\tau)$ for a Laguerre-Gauss (LG) beam. From (3:4), the electromagnetic interaction perturbation Hamiltonian for a particle *n* is:

$$\hat{H}_n^{(1)} = -i\mu_{Bn}\left[\vec{A}(\vec{r}_n,t)\bullet\nabla_n + \nabla_n\bullet\vec{A}(\vec{r}_n,t) + \vec{s}_n\bullet\nabla_n\times\vec{A}(\vec{r}_n,t)\right] \qquad (3:11)$$

Apply a variable separation (time) for the equations describing the LG wave (1:10 – 1:14):

$$\begin{aligned}
&\mathsf{F}_{l,p}\left(\vec{r}_n\right) = A_{pol,\rho} f_{l,p}\left(\rho_n\right) e^{i(kz_n - l\theta_n)} \\
&\vec{A}\left(\vec{r}_n, t\right) = \mathsf{F}_{l,p}\left(\vec{r}_n\right) e^{-i\omega t}\vec{\mathbf{1}}_\rho \\
&\vec{B}\left(\vec{r}_n, t\right) = i\,\mathsf{F}_{l,p}\left(\vec{r}_n\right)\left(-k\vec{\mathbf{1}}_\theta + \frac{l}{\rho_n}\vec{\mathbf{1}}_z\right) e^{-i\omega t}
\end{aligned} \tag{3:12}$$

Since the field is not uniform, the Coulomb Gauge does not apply:

$$\nabla_n \cdot \vec{A}\left(\vec{r}_n, t \neq 0\right) \tag{3:13}$$

After some algebra involving the expression for ∇_n in cylindrical coordinates, the Hamiltonian operator becomes:

$$\hat{H}_n^{(1)}(t) = \hat{\mathsf{H}}_n^{(1)} e^{-i\omega t} = -i\mu_n \mathsf{F}_{l,p}\left(\vec{r}_n\right)\left[\frac{\partial}{\partial\rho_n} + \frac{1}{\mathsf{F}_{l,p}\left(\vec{r}_n\right)}\frac{\partial \mathsf{F}_{l,p}\left(\vec{r}_n\right)}{\partial\rho_n} + k\vec{s}_n \bullet \vec{\mathbf{1}}_\theta - \frac{l}{\rho_n}\vec{s}_n \bullet \vec{\mathbf{1}}_z\right] e^{-i\omega t} \tag{3:14}$$

$\hat{\mathsf{H}}_n^{(1)}$ is the time independent operator associated to the perturbed Hamiltonian. From (3:9) and (3:15) one can find the value of the transition probability as:

$$c_b(t) = \frac{1}{i\hbar}\sum_{n=1}^{n_{mol}}\int_0^\infty\left(\left\langle b\middle|H_n^{(1)}\middle|a\right\rangle\int_0^t e^{i(\omega_{ba}-\omega)\tau}\,d\tau + h.c.\right)d\omega \tag{3:15}$$

h.c. is the complex harmonic conjugate of the transition matrix:

$$h.c. = \left\langle b\middle|H_n^{(1)^*}\middle|a\right\rangle\int_0^t e^{i(\omega_{ba}+\omega)\tau}\,d\tau + h.c. \tag{3:16}$$

Photon absorption occurs when the final energy of the molecule exceeds the initial value ($\omega_{ba} \geq 0$). This condition nulls the *h.c.* term. The transition probability for absorption is proportional to:

$$\left\|c_b(t)\right\|^2 = \left\|\frac{1}{\hbar}\sum_{n=1}^{n_{mol}}\int_0^\infty\left\langle b\middle|H_n^{(1)}\middle|a\right\rangle\int_0^t e^{i(\omega_{ba}-\omega)\tau}\,d\tau.d\omega\right\|^2 \tag{3:17}$$

We can simplify this expression further, by observing that the absolute value of the exponential function integral in (3:17) is approximately null except for frequencies close to ω_{ba}. The matrix element in the previous formula has meaningful values only around $\omega \quad \omega_{ba}$:

$$\left\|c_b(t)\right\|^2 = \left\|\frac{1}{\hbar}\sum_{n=1}^{n_{mol}}\int_0^\infty\left\langle b\middle|H_n^{(1)}\middle|a\right\rangle\int_0^t e^{i(\omega_{ba}-\omega)\tau}\,d\tau.d\omega\right\|^2 \tag{3:18}$$

The time and frequency double integral yields:

$$\left\| \int_{-\infty}^{\infty} \int_{0}^{t} e^{i(\omega_{ba}-\omega)\tau} \, d\tau . d\omega \right\|^2 = \pi t \qquad (3:19)$$

We then obtain a general result: the probability for the system to be in the state *b* at time *t*, assuming that *a* is the initial state of the system equals:

$$\left\| c_b(t) \right\|^2 = \frac{\pi}{\hbar^2} \left\| \sum_{n=1}^{n_{mol}} \left\langle b \left| H_n^{(1)} \right| a \right\rangle \Big|_{\omega=\omega_{ba}} \right\|^2 t \qquad (3:20)$$

With (3:1), the transition rate is:

$$W_{fi} = \frac{dP_{fi}}{dt} = h \left| V_{fi} \right|^2 D\left(E_{fi}\right) = \frac{2\pi^2}{\hbar} \left\| \sum_{n=1}^{n_{mol}} \left\langle f \left| H_n^{(1)} \right| i \right\rangle \Big|_{\omega=\omega_{fi}} \right\|^2 D\left(E_{fi}\right) \qquad (3:21)$$

Therefore, the matrix element is expressed for every particle involved in the photon absorption process, and the absolute value of their sum is calculated.

The matrix element for particle *n* (first order perturbation theory) is:

$$M_{n,f\leftarrow i,l,p} = -i\mu_n \left\langle f \left| \mathsf{F}_{l,p}\left(\vec{r}_n\right) \left(\frac{\partial}{\partial \rho_n} + \frac{1}{\mathsf{F}_{l,p}\left(\vec{r}_n\right)} \frac{\partial \mathsf{F}_{l,p}\left(\vec{r}_n\right)}{\partial \rho_n} + k\vec{s}_n \bullet \vec{\mathbf{1}}_\theta - \frac{l}{\rho_n} \vec{s}_n \bullet \vec{\mathbf{1}}_z \right) \right| i \right\rangle \qquad (3:22)$$

This result is exact.

Theory: Transition matrix interpretation

The matrix element is a sum of 4 terms:

$$\begin{aligned} M^{I}_{n,f\leftarrow i,l,p} &= -i\mu_n \left\langle f \left| \mathsf{F}_{l,p}\left(\vec{r}_n\right) \frac{\partial}{\partial \rho_n} \right| i \right\rangle \\ M^{II}_{n,f\leftarrow i,l,p} &= -i\mu_n \left\langle f \left| \frac{\partial \mathsf{F}_{l,p}\left(\vec{r}_n\right)}{\partial \rho_n} \right| i \right\rangle \\ M^{III}_{n,f\leftarrow i,l,p} &= -i\mu_n k \left\langle f \left| \mathsf{F}_{l,p}\left(\vec{r}_n\right) \vec{s}_n \bullet \vec{\mathbf{1}}_\theta \right| i \right\rangle \\ M^{IV}_{n,f\leftarrow i,l,p} &= i\mu_n l \left\langle f \left| \frac{\mathsf{F}_{l,p}\left(\vec{r}_n\right)}{\rho_n} \vec{s}_n \bullet \vec{\mathbf{1}}_z \right| i \right\rangle \end{aligned} \qquad (4:1)$$

Transition $M^{I}_{n,f\leftarrow i,l,p}$

The first term, $M^{I}_{n,f\leftarrow i,l,p}$ describes the kinetic energy contribution of a particle.

$$\left.\begin{aligned} &\mathsf{F}_{l,p}\left(\vec{r}_n\right)=f_{l,p}\left(\rho_n\right)e^{i(kz_n-l\theta_n)}\\ &M^{I}_{n,f\leftarrow i,l,0}=-i\mu_n\left\langle f\left|\mathsf{F}_{l,p}\left(\vec{r}_n\right)\frac{\partial}{\partial\rho_n}\right|i\right\rangle \end{aligned}\right\}\Rightarrow$$

$$\left.\begin{aligned} &M^{I}_{n,f\leftarrow i,l,p}=-i\mu_n\left\langle f\left|f_{l,p}\left(\rho_n\right)e^{i(kz_n-l\theta_n)}\frac{\partial}{\partial\rho_n}\right|i\right\rangle\\ &e^{i(kz_n-l\theta_n)}=e^{-il\theta_n}\sum_{q=0}^{\infty}\frac{1}{q!}(ikz_n)^q\approx e^{-il\theta_n} \end{aligned}\right\}\Rightarrow \qquad (4:2)$$

$$M^{I}_{n,f\leftarrow i,l,0}=-i\mu_n\left\langle f\left|f_{l,p}\left(\rho_n\right)e^{-il\theta_n}\frac{\partial}{\partial\rho_n}\right|i\right\rangle$$

$M^{I}_{n,f\leftarrow i,l,0}$ is proportional to $f_{l,0}(\rho)=\frac{1}{w_0}\left(\frac{\rho}{w_0}\right)^{|l|}e^{-\left(\frac{\rho}{w_0}\right)^2}$ and the non-uniformity of the molecule in the plane perpendicular to the beam propagation.

Let us observe the influence of w_0, which represents the beam waist:

- for a large w_0, $\lim_{w_0\to\infty}\left(M^{I}_{n,f\leftarrow i,l,0}\right)\to 0$;
- for small w_0, $\lim_{w_0\to 0}\left(M^{I}_{n,f\leftarrow i,l,0}\right)\to 0$;
- maximum of $M^{I}_{n,f\leftarrow i,l,0}$ occurs for $\frac{\partial M^{I}_{n,f\leftarrow i,l,0}}{\partial w_0}=0$ at $w_0=\rho\sqrt{2/\left(1+|l|\right)}$; and
- maximum of $M^{I}_{n,f\leftarrow i,l,0}$ occurs for $\frac{\partial M^{I}_{n,f\leftarrow i,l,0}}{\partial \rho}=0$ at $\rho=w_0\sqrt{l/2}$.

One could conclude that the maximum observable effect area is given by the Airy disk:

1. The probability of OAM interaction with molecules is zero at spatial points placed far from the centre of the light beam or in the centre of the light beam.
2. The probability of OAM interaction with molecules reaches maximum at spatial points placed at $\rho=w_0\sqrt{l/2}$.
3. The probability of OAM interaction with molecules reaches maximum at spatial points placed at $w_0=\rho\sqrt{2/\left(1+|l|\right)}$.
4. Maximum interaction probability occurs on the radius corresponding to the maximum field distribution, for circles close to the Airy disk.

Transition $M^{II}_{n,f\leftarrow i,l,p}$

The second term, $M^{II}_{n,f\leftarrow i,l,p}$

$$\left.\begin{aligned} M^{II}_{n,f\leftarrow i,l,p} &= -i\mu_n \left\langle f \left| \frac{\partial \mathsf{F}_{l,p}\left(\vec{r}_n\right)}{\partial \rho_n} \right| i \right\rangle \\ \mathsf{F}_{l,p}\left(\vec{r}_n\right) &= f_{l,p}\left(\rho_n\right) e^{i(kz_n - l\theta_n)} \end{aligned}\right\} \Rightarrow$$
$$M^{II}_{n,f\leftarrow i,l,p} = -i\mu_n \left\langle f \left| \frac{\partial f_{l,p}\left(\rho_n\right)}{\partial \rho_n} e^{i(kz_n - l\theta_n)} \right| i \right\rangle \qquad (4:3)$$

$f_{l,p}\left(\rho_n\right)$ is given by (1:8) with $R_n = \sqrt{2}\rho_n / w_0$. The radial derivative of $f_{l,p}\left(\rho_n\right)$ is:

$$\frac{\partial f_{l,p}\left(\rho_n\right)}{\partial \rho_n} = \frac{C_{l,p}}{w_0} \frac{\partial \left(R_n^{|l|} e^{-\left(\frac{R_n}{\sqrt{2}}\right)^2} L_p^{|l|}\left(R_n^2\right) \right)}{\partial R_n} \frac{\partial R_n}{\partial \rho_n} \Leftrightarrow$$
$$\frac{\partial f_{l,p}\left(\rho_n\right)}{\partial \rho_n} = \frac{C_{l,p}}{w_0} \frac{\sqrt{2}}{w_0} \left(\frac{|l|}{R_n} R_n^{|l|} e^{-\left(\frac{R_n}{\sqrt{2}}\right)^2} L_p^{|l|}\left(R_n^2\right) - R_n R_n^{|l|} e^{-\left(\frac{R_n}{\sqrt{2}}\right)^2} L_p^{|l|}\left(R_n^2\right) + R_n^{|l|} e^{-\left(\frac{R_n}{\sqrt{2}}\right)^2} \frac{\partial L_p^{|l|}\left(R_n^2\right)}{\partial R_n} \right) \qquad (4:4)$$

From orthogonal polynomial recurrence properties one can calculate the derivative for a Laguerre polynomial as:

$$\frac{\partial L_p^{|l|}\left(R_n^2\right)}{\partial R_n} = \frac{2}{R_n} \left(p L_p^{|l|}\left(R_n^2\right) - \left(p + |l|\right) L_{p-1}^{|l|}\left(R_n^2\right) \right) \qquad (4:5)$$

Replacing the latest in the formula for $f_{l,p}\left(\rho_n\right)$ radial derivative we obtain:

$$\frac{\partial f_{l,p}\left(\rho_n\right)}{\partial \rho_n} = f_{l,p}\left(\rho_n\right) \frac{\sqrt{2}}{w_0} \frac{1}{R_n} \left(|l| + 2p - R_n^2 - 2\left(|l| + p\right) \frac{L_{p-1}^{|l|}\left(R_n^2\right)}{L_p^{|l|}\left(R_n^2\right)} \right) \qquad (4:6)$$

Using Laguerre polynomial recurrence definition (1:8) we express the order *p-1* as a function of order *p:*

$$L_p^{|l|}\left(R_n^2\right) = \sum_{m=0}^{p-1} (-1)^m \frac{\left(p + |l|\right)!}{(p-m)!\left(|l| + m\right)! m!} R_n^{2m} + (-1)^p \frac{\left(p + |l|\right)!}{(p-p)!\left(|l| + p\right)! p!} R_n^{2p} \Leftrightarrow$$
$$\frac{L_{p-1}^{|l|}\left(R_n^2\right)}{L_p^{|l|}\left(R_n^2\right)} = 1 - \frac{(-1)^p}{p!} \frac{R_n^{2p}}{L_p^{|l|}\left(R_n^2\right)} \qquad (4:7)$$

This finally leads to:

$$\frac{\partial f_{l,p}(\rho_n)}{\partial \rho_n} = f_{l,p}(\rho_n)\frac{\sqrt{2}}{w_0}\frac{1}{R_n}\left(|l|+2p-R_n^2-2(|l|+p)\left(1-\frac{(-1)^p}{p!}\frac{R_n^{2p}}{L_p^{|l|}(R_n^2)}\right)\right) \quad \Leftrightarrow$$
$$\frac{\partial f_{l,p}(\rho_n)}{\partial \rho_n} = f_{l,p}(\rho_n)\frac{\sqrt{2}}{w_0}\left(-\frac{|l|}{R_n}-R_n+\frac{(-1)^p\,2(|l|+p)}{p!}\frac{R_n^{2p-1}}{L_p^{|l|}(R_n^2)}\right) \qquad (4:8)$$

The matrix element is:

$$M^{II}_{n,f\leftarrow i,l,p} = i\mu_n\frac{\sqrt{2}}{w_0}\left[-|l|\left\langle f\left|\frac{\mathbf{F}_{l,p}(\vec{r}_n)}{R_n}\right|i\right\rangle-\left\langle f\left|R_n\,\mathbf{F}_{l,p}(\vec{r}_n)\right|i\right\rangle+\right.$$
$$\left.\frac{(-1)^p\,2(|l|+p)}{p!}\left\langle f\left|\frac{R_n^{2p-1}}{L_p^{|l|}(R_n^2)}\mathbf{F}_{l,p}(\vec{r}_n)\right|i\right\rangle\right] \qquad (4:9)$$

Let's simplify it for the particular case of $p = 0$:

$$M^{II}_{n,f\leftarrow i,l,0} = i\mu_n\frac{\sqrt{2}}{w_0}\left(|l|\langle f|\frac{\mathsf{F}_{l,0}(\vec{r}_n)}{R_n}|i\rangle-\langle f|R_n\mathsf{F}_{l,0}(\vec{r}_n)|i\rangle\right) \qquad (4:10)$$

It shows the matrix element $M^{II}_{n,f\leftarrow i,l,p}$ is linearly dependent on l.

Transition $M^{III}_{n,f\leftarrow i,l,p}$

The third term is:

$$M^{III}_{n,f\leftarrow i,l,p} = -i\mu_n k\left\langle f\left|\mathsf{F}_{l,p}(\vec{r}_n)\vec{s}_n\bullet\vec{\mathbf{1}}_\theta\right|i\right\rangle \qquad (4:11)$$

The matrix element $M^{III}_{n,f\leftarrow i,l,p}$ represents the interaction of the OAM with electron (and nucleon) spin.

Transition $M^{IV}_{n,f\leftarrow i,l,p}$

The fourth term is of a major interest, since it depicts a linear dependence of a transition probability on a parameter of the incident light, other than frequency or spin:

$$M^{IV}_{n,f\leftarrow i,l,p} = i\mu_n l\left\langle f\left|\frac{\mathsf{F}_{l,p}\left(\vec{r}_n\right)}{\rho_n}\vec{s}_n \bullet \vec{\mathbf{1}}_z\right|i\right\rangle = i\mu_n l\left\langle f\left|\frac{\mathsf{F}_{l,p}\left(\vec{r}_n\right)}{\rho_n}\left(\vec{L}_n + \vec{\sigma}_n\right)\bullet \vec{\mathbf{1}}_z\right|i\right\rangle$$
$$= i\mu_n l\left(\left\langle f\left|\frac{\mathsf{F}_{l,p}\left(\vec{r}_n\right)}{\rho_n}\vec{L}_n \bullet \vec{\mathbf{1}}_z\right|i\right\rangle + \left\langle f\left|\frac{\mathsf{F}_{l,p}\left(\vec{r}_n\right)}{\rho_n}\vec{\sigma}_n \bullet \vec{\mathbf{1}}_z\right|i\right\rangle\right) \qquad (4:12)$$
$$= i\mu_n l\left(\left\langle f\left|M^{II}_{n,f\leftarrow i,l,p} L_{n,\vec{\mathbf{1}}_z}\right|i\right\rangle + \left\langle f\left|\frac{\mathsf{F}_{l,p}\left(\vec{r}_n\right)}{\rho_n}\vec{\sigma}_n \bullet \vec{\mathbf{1}}_z\right|i\right\rangle\right)$$

$M^{IV}_{n,f\leftarrow i,l,p}$ shows that there is an interaction of the light carrying OAM with the kinetic momentum $L_{n,\vec{\mathbf{1}}_z}$ component parallel to the direction of the light beam $\vec{\mathbf{1}}_z$. This interaction is proportional to the OAM of light l and is more probable for low ρ_n (beam waist close to the minimum of the diffraction limited Airy disk). Same comments apply for the interaction of light carrying spin $\vec{\sigma}_n$ with the electron magneton.

This is the basis for producing fluid with hyperpolarization along the direction $\vec{\mathbf{1}}_z$ of the propagation of the light beam.

- The formulae above show that there is an interaction of the momenta carried by light with all types of spins and orbital momenta carried by molecule constituents.
- The same formulae also show that in some cases, the transition matrix coefficients are proportional to l, therefore a higher interaction is probable for light carrying large OAM.
- The transition matrix coefficients $M^{II}_{n,f\leftarrow i,l,p}$ and $M^{IV}_{n,f\leftarrow i,l,p}$ include terms proportional to $\frac{1}{R_n}$ and $\frac{1}{\rho_n}$, meaning that these coefficients reach higher values for small R_n and ρ_n. Given the "maximum observable effect area" criteria from the previous section, the maximum value of the transition matrix coefficients $M^{II}_{n,f\leftarrow i,l,p}$ and $M^{IV}_{n,f\leftarrow i,l,p}$ is obtained with a light beam with the radius as close as possible to the Airy disk radius.
- These coefficients apply for photon – molecule absorption, emission and quasi-transitions.
- These coefficients refer to the gross selection rules, which are statements about the properties that a molecule must possess in order for it to be capable of showing a particular type of transition.

The specific selection rules (the changes in quantum numbers that may occur during such transitions) are not predicted by this theory, but are qualitatively mentioned in Figure 4.

Specific selection rules for molecule-light interactions

Absorption

Light carrying spin $\vec{\sigma}_n$ and OAM l is absorbed by molecules. As angular momentum is a conserved quantity, the total angular momentum of the system (radiation and matter) cannot be changed during absorption and emission of radiation. When a photon is absorbed by an atom or molecule, its angular momentum has to be therefore transferred to the atom. The resulting angular momentum of the atom then equals to the vector sum of its initial angular momentum plus the angular momentum of the absorbed photon.

Atoms and molecules may contain different types of angular momenta. The most important reservoirs include orbital angular momentum of electrons, rotational motion of molecules and spin angular momentum of electrons and nuclei. Not all these types of angular momenta couple directly to the radiation field: in free atoms, only the orbital angular momentum of the electrons is directly coupled to the optical transitions. However, the different types of angular momenta are in general coupled to each other by various interactions which allow the polarization to flow from the photon spin reservoir through the electron orbital to all the other reservoirs, as shown schematically in Figure 4.

Above it was demonstrated theoretically the possibility of OAM – molecule interaction that made possible the OAM-rotation transitions shown in Figure 4. It was also demonstrated that the interaction is proportional to the value of the OAM carried by the light beam.

Therefore, it is probable (proportional to l) to:

- Transfer/align not only the electronic spin population of orbitals excited during absorption processes, but also the OAM of the molecule.
- Change the molecular rotation value and orientation towards momenta parallel to the beam axis propagation (on the periphery of the Airy disk).
- Direct transfer/align molecule nuclei.

Transparent molecules

These are cases of "quasi-transitions", where photons interact with orbitals, but do not have enough energy to produce an excited molecular state. The photon is absorbed and emitted by the molecule almost at the same time (short "quasi-state" life time). There are changes within the incident and emitted photons momenta and energies (e.g. Raman back

scattering). Therefore, light with OAM will interact with transparent molecules as well, transferring the photon angular momenta to the rotational momentum of the molecule.

We can conclude that molecules' momenta are changed, i.e. aligned in direction to the incident beam propagation axis and modified in magnitude, by light endowed with spin and OAM, proportional to the OAM content of light.

The optical pumping shows that molecules can be hyperpolarized with light carrying spin (circular polarized light). The method has been successfully used for obtaining hyperpolarized gases, with applications in MRI.

The present invention adds the photons an OAM, therefore increases the orientation of the molecular momenta along the direction of propagation of the light and increases the probability of obtaining hyperpolarized molecules within fluids. Hence, an NMR analysis of the fluid is possible.

This concept has been experimentally proven by a laboratory setup, which will be described next.

Laboratory setup description

Figure 5 shows an exemplary setup of a measurement system 500 for analyzing a blood sample in accordance with the teachings of the present invention. The white light is produced with an HP Mercury, 100W white light source 501, and is collimated so that the diameter of the beam is roughly 1mm. The collimated light, i.e. the beam, is then sent to a beam expander (1:20) 503. After passing through the beam expander 503, the light is circularly polarized with a linear polarizer 505 followed by a quarter wave plate 507.

A holographic plate 509 is provided for producing the desired type of light endowed with OAM and possibly spin. The value l of the OAM is a parameter of the holographic plate and can be increased to values up to 40, but cannot be easily further increased due to practical issues related to spatial filtering. The spatial filter 511 is used for discriminating the light confining the OAM from the rest of the diffracted light generated by the holographic filter 509.

The dispersed diffracted beams are collected and focused onto the sample by use of concave mirrors 513 and a fast microscope objective 515. The high $f_{\#}$ is required in order to satisfy the condition of a beam waist as close as possible to the Airy disk size.

After passing through the objective 515, a tightly focused beam of white light carrying spin (circular polarization) and an OAM of $l = 19$ was obtained. The beam is then applied to a blood vessel through a hole in a CMOS MEMS device 517, which is next explained in more detail.

The CMOS MEMS device 517 confines an NMR CMOS processing unit 601 shown in further detail in Figure 6 and an NMR fluid sample interface.

The NMR CMOS processing unit circuitry 601 contains the following blocks:

- 10MHz maximum bandwidth low noise amplifier (LNA) 603 having maximum sensitivity around 1μV and maximum programmable gain of 60dB, and of which purpose is to amplify the signals provided by receiving coils 604. The purpose of the receiving or measurement coils 604 is to measure the obtained FID signal.
- 10MHz maximum bandwidth transimpedance amplifiers 605 (programmable gain amplifiers, PGAs, in Figure 6) with programmable gain to supply the pulse sequences required for NMR FID.
- Analog CMOS multiplexers 607, to connect the coils 604 to the output of the transimpedance amplifiers 605 or LNA 603 input.
- Pulse generator 609 to provide multiple output voltage pulses with programmable amplitudes and spectral composition. The pulses are applied at the inputs of the transimpedance amplifiers 605.
- Analog-to-digital (AD) converter 611 with a resolution of 12 – 16 bits, 20Ms/s, to convert the FID sequences received from the coils 604.
- A memory 612 for storing data.
- A digital signal processor (DSP) 613 to produce the FFT data set corresponding to every digitized FID sequence.
- XTal driven fractional frequency synthesizer/PLL (frequency control unit in Figure 6) 616, to generate reference clocks.
- A control unit 615 to control the general functioning of the NMR CMOS processing unit 601.
- White light source controller 617 to generate all signals required for the operation of the white light source.
- Input-output (IO) unit 619, for external device data transfers.

After the CMOS MEMS processing device 601 has been manufactured, MEMS processes continue the processing of the die according to the following macros:

- Deposit, pattern and etch a thick dielectric film 701 as the base for the multiple coils to be placed on top of the structure.
- Deposit, pattern and etch vias and metal connectivity required to connect the CMOS circuitry with the top coils 702. The purpose of the top coils 702 is to create a sequence of magnetic fields for realigning the nuclei once they have been aligned by use of light with OAM.

- Manufacture (using existing MEMS processes) the top coils 702, as shown in an arrangement similar to the one given in Figure 7.
- Deposit, pattern and etch a dielectric protective layer 703, to cover the manufactured coils 702.
- Etch a circular hole 705 through the entire device 517 as shown in Figure 7 that allows the propagation of light through the device 517. The circular hole is especially advantageous because it maintains the symmetry of the signals received by the coils 604 after an FID sequence has been generated.
- Glue the structure on chemical inactive transparent glass 707, which is transparent for incident light.

The CMOS MEMS device 517 is placed adjacent to the objective 515 as is shown in Figure 5. The light emerging from a fast lens of the objective 515 shall be focused in the centre of the coil system. The OAM beam focused spot is around 5 m in diameter. In this example the diameter of the hole is around 100 m in and all coil inner diameters shall not exceed 50 m.

Experiment flow description

The setup described above allows the acquisition of the magnetic FID of a sample illuminated with light with spin and an OAM of $10\hbar$ and comparing it with the same FID coming from the not illuminated sample. The last case might seem unnecessary, since the FID of an unpolarized sample shall produce amplitudes below the noise level of the acquisition system. However, generating the difference between the illuminated and "dark" sample is beneficial in order to reduce all ergodic environment noise sources.

One embodiment of a method of performing a high resolution fluid analysis is described next with reference to the flow chart of Figure 8. First in step 801 the measurement system 500 is placed in close proximity to the blood vessel so that the system 500 is within an operating range of the blood vessel. Then in step 803 the light source 501 is turned on. Next in step 805 the light acquires OAM and possibly spin once it passes through the polarizer 505, quarter wave plate 507 and holographic plate 509.

Then in step 807, the light beam is focused onto the sample by using the concave mirrors 513 and microscope objective 515. When the light is applied to the sample, nuclei will get oriented (precession movement) around the light beam propagation axis. This process shall produce a detectable FID signal, which shall reflect in peaks within the FID spectrum for the positive edge triggered acquisition, positive edge corresponding to the event "light start passing through the sample". The measurement coils 604 serve as an FID

detector. In step 809 the light is sequentially switched on and off for obtaining (step 813) the FID signal. To have a more controlled FID signal, in step 813 a sequence of magnetic fields is created by the top coils 702. These magnetic fields are perpendicular to the direction of the light. When the light is turned off, the magnetic field is created and the thermal nuclei shall relax their orientation, and will get oriented to be more or less aligned with the magnetic field. Thus, the nuclei get oriented into two directions, the first direction being determined by the direction of the light and the second direction being determined by the direction of the magnetic field. In this example the pulse period is about 70ms and the duty factor is 50%. The applied magnetic field can be a static field or it can be an RF field that is tuned to interact more strongly with specific nuclei. Alternatively this can be done by applying another light beam perpendicular to the first beam. Finally, in step 815 the obtained FID signal is measured by the measurement coils 604.

More evolved experimental setups require perpendicular coils for different NMR FID excitation sequences, a more efficient method to produce white light and means to modify the light spectrum that is sent to the sample, a more efficient way to modulate the OAM and a better data acquisition (longer acquisition sequences, higher data rates at higher sensitivities) system.

Above an embodiment was described. The invention is applicable in all situations where non-invasive blood analysis is required, given the restriction of the availability of a shallow blood vessel. The invention can for instance be used for non-invasive glucose monitoring for diabetic patients.

The invention equally relates to a computer program product that is able to implement any of the method steps of the embodiments of the invention when loaded and run on computer means of the analysis device mentioned above. A computer program may be stored/distributed on a suitable medium supplied together with or as a part of other hardware, but may also be distributed in other forms, such as via the Internet or other wired or wireless telecommunication systems.

The present invention equally relates to an integrated circuit that is arranged to perform any of the method steps in accordance with the embodiments of the invention.

While the invention has been illustrated and described in detail in the drawings and foregoing description, such illustration and description are to be considered illustrative or exemplary and not restrictive; the invention is not restricted to the disclosed embodiments.

Other variations to the disclosed embodiments can be understood and effected by those skilled in the art in practicing the claimed invention, from a study of the drawings, the disclosure and the appended claims. In the claims, the word “comprising” does not exclude

other elements or steps, and the indefinite article "a" or "an" does not exclude a plurality. A single processor or other unit may fulfill the functions of several items recited in the claims. The mere fact that different features are recited in mutually different dependent claims does not indicate that a combination of these features cannot be advantageously used. Any reference signs in the claims should not be construed as limiting the scope of the invention.

CLAIMS

1. A non-invasive method of analyzing a fluid sample consisting of molecules, the analysis being based upon nuclear magnetic resonance spectroscopy, the method comprising the following steps:

- placing (801) an analysis device (517) within an operation range of the sample to be analyzed;
- operating (803; 805; 807) in a non-invasive manner the analysis device (517) for obtaining localized nuclear magnetic polarizability of the sample to align nuclei of the molecules to a first direction;
- relaxing (809) the nuclei to realign them to a second direction and then sequentially (809; 811) aligning and realigning the nuclei to said first and second directions, respectively, for obtaining a free induction decay magnetic signal containing information about the sample; and
- measuring (815) the obtained free induction decay magnetic signal for analyzing the sample.

2. The method according to claim 1, wherein operating the analysis device (517) comprises:

- turning on (803) a light source (501);
- introducing (805) orbital angular momentum into the light;
- obtaining (807) a focused light beam carrying orbital angular momentum; and
- illuminating (807) the sample with the focused light beam carrying orbital angular momentum for aligning the nuclei to said first direction.

3. The method according to claim 2, wherein the light beam is also endowed with angular momentum.

4. The method according to any one of claims 2-3, wherein the free induction decay signal is obtained by applying (809) to the sample a sequence of light pulses for obtaining the sequential alignment of the nuclei resulting from the sequential illumination of the sample.

5. The method according to any one of claims 2-4, further comprising applying to the sample at least one of the following: a magnetic field essentially perpendicular to the light

beam, radio frequency field tuned to interact more strongly with specific nuclei and/or a second light beam for rotating the light beam to obtain the alignment of the magnetons in said second direction.

6. The method according to any of the preceding claims, further comprising comparing the free induction decay signal corresponding to the sample in nuclear magnetic polarized state with another free induction signal corresponding to a sample in non nuclear magnetic polarized state.

7. The method according to any one of claims 2-6, wherein the nuclear magnetic polarizability of the sample is achieved by the molecules absorbing photons carried by the light thereby transferring to the interacting molecules the orbital angular momentum of the light.

8. The method according to any of the preceding claims, wherein for obtaining the nuclear magnetic polarizability of the sample no magnet is employed.

9. A computer program product for a fluid analysis device, the program comprising instructions for implementing the steps of a method according to any one of claims 1 through 8 when loaded and run on computer means of an analysis device (517).

10. A non-invasive analysis device (517) for analyzing a fluid sample consisting of molecules, the analysis being based upon nuclear magnetic resonance spectroscopy, the device comprises:

- means (617) for obtaining in a localized space nuclear magnetic polarizability of the sample to align magnetons of the molecules to a first direction;
- means (617; 702) for relaxing the magnetons to realign them to a second direction;
- means (617; 702) for sequentially aligning and realigning the magnetons to said first and second directions, respectively, for obtaining a free induction decay magnetic signal containing information about the sample; and
- means (604) for measuring the obtained free induction decay magnetic signal for analyzing the sample.

11. The device according to claim 10, further comprising at least two coils (702) arranged to create a sequence of magnetic fields for realigning the magnetons to said second direction.

12. The device according to any one of claims 10-11, comprising a hole (705) through which a light pulse is arranged to be directed to the sample, said hole (705) being surrounded by coils (702).

13. The device according to any one of claims 10-12, further comprising a Fourier transformation unit (613) for transforming the free induction decay signal into frequency domain signal.

14. The device according to any one of claims 10-13 further comprising at least one measurement coil (604) for measuring the free induction decay signal.

15. A measurement system comprising the non-invasive analysis device (517) according to any one of claims 10-14, wherein the measurement system further comprises:

- a light source (501) for creating light;
- means (509) for introducing orbital angular momentum into the light;
- means (513) for obtaining a focused light beam; and
- means (515) for illuminating the sample with the focused light beam carrying orbital angular momentum for obtaining nuclear magnetic polarizability of the sample.

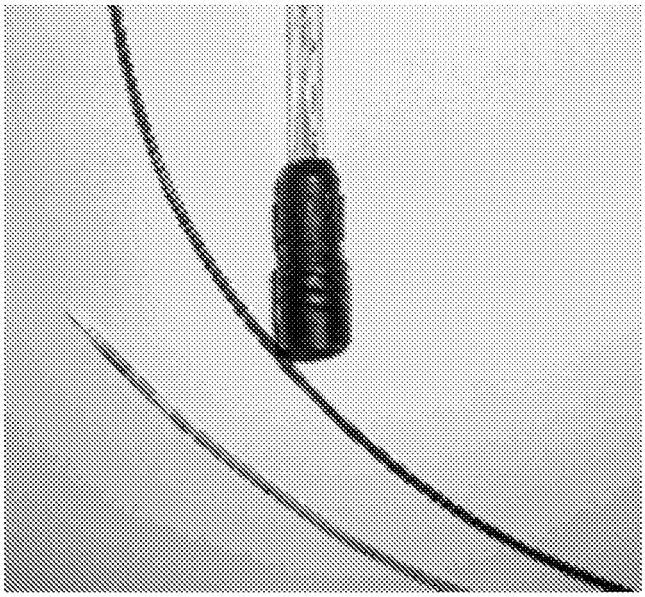

FIG. 1

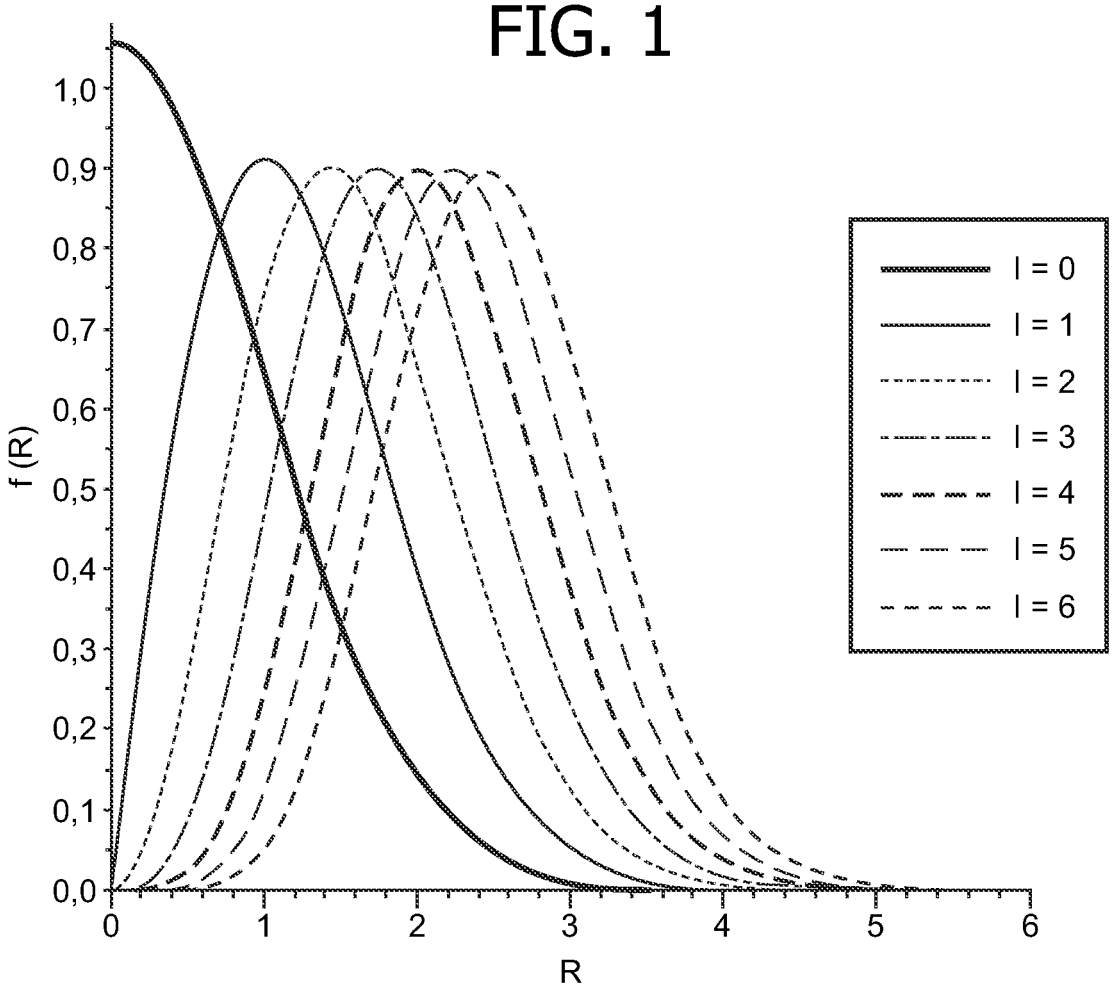

FIG. 2

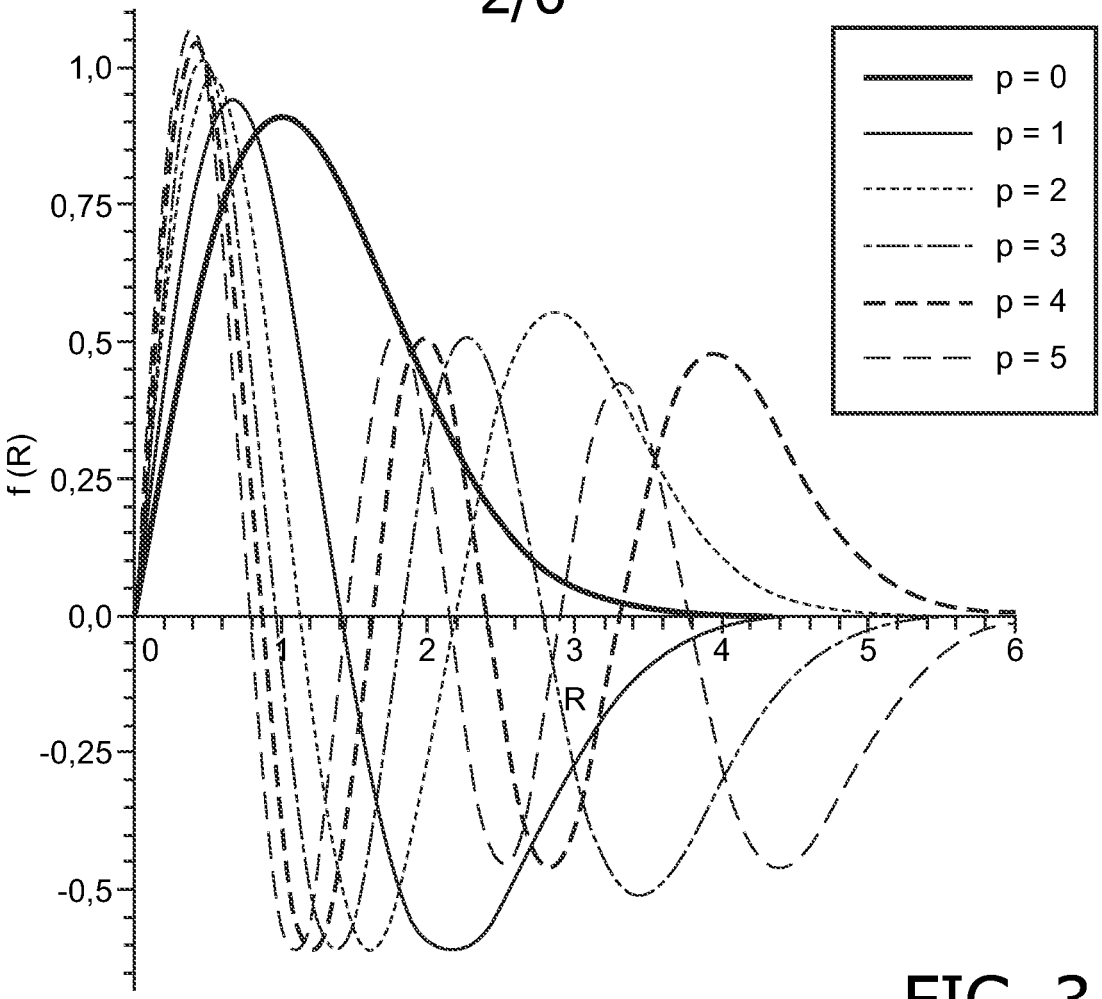
1,0
0,75
0,5
0,25
0,0
-0,25
-0,5
f (R)
0
1
2
3
4
5
6
R
p = 0
p = 1
p = 2
p = 3
p = 4
p = 5

FIG. 3

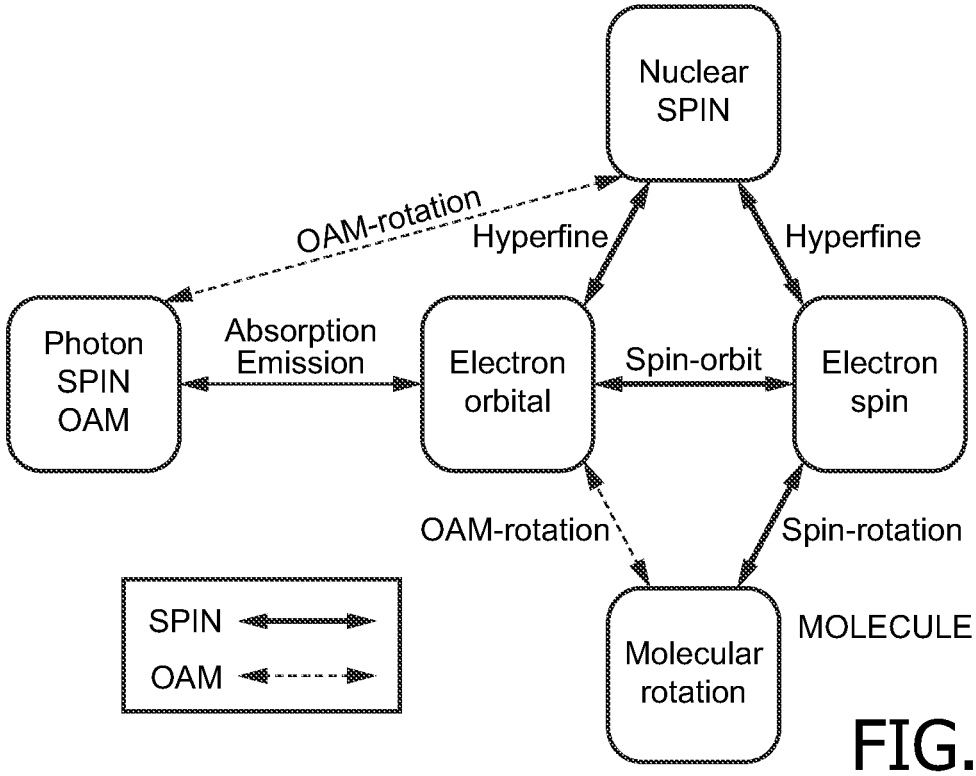
Nuclear SPIN
OAM-rotation
Hyperfine
Hyperfine
Photon SPIN OAM
Absorption Emission
Electron orbital
Spin-orbit
Electron spin
OAM-rotation
Spin-rotation
Molecular rotation
MOLECULE
SPIN
OAM

FIG. 4

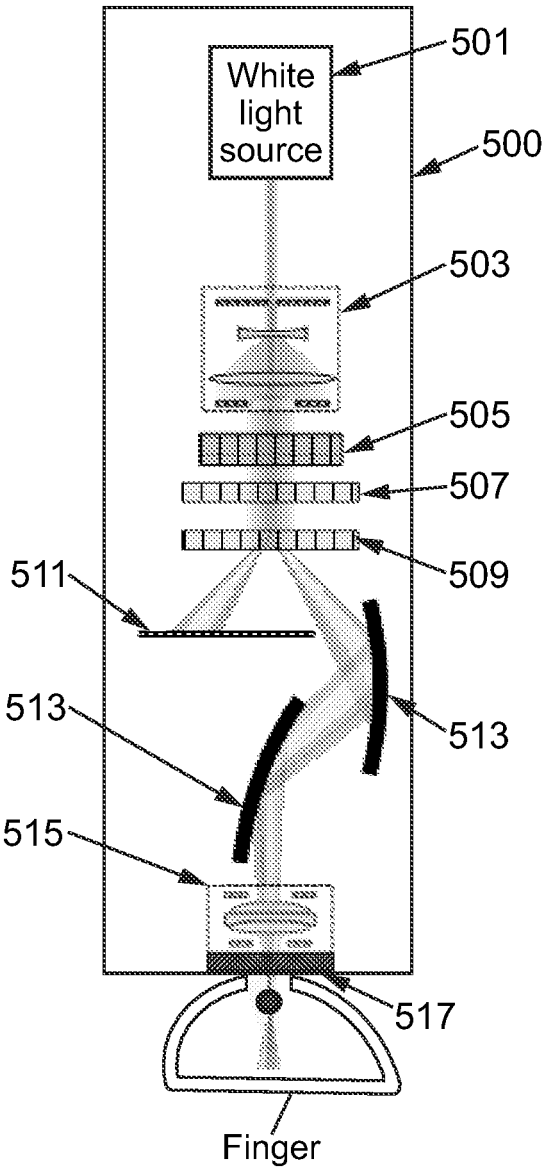
White light source
501
500
503
505
507
509
511
513
513
515
517
Finger

FIG. 5

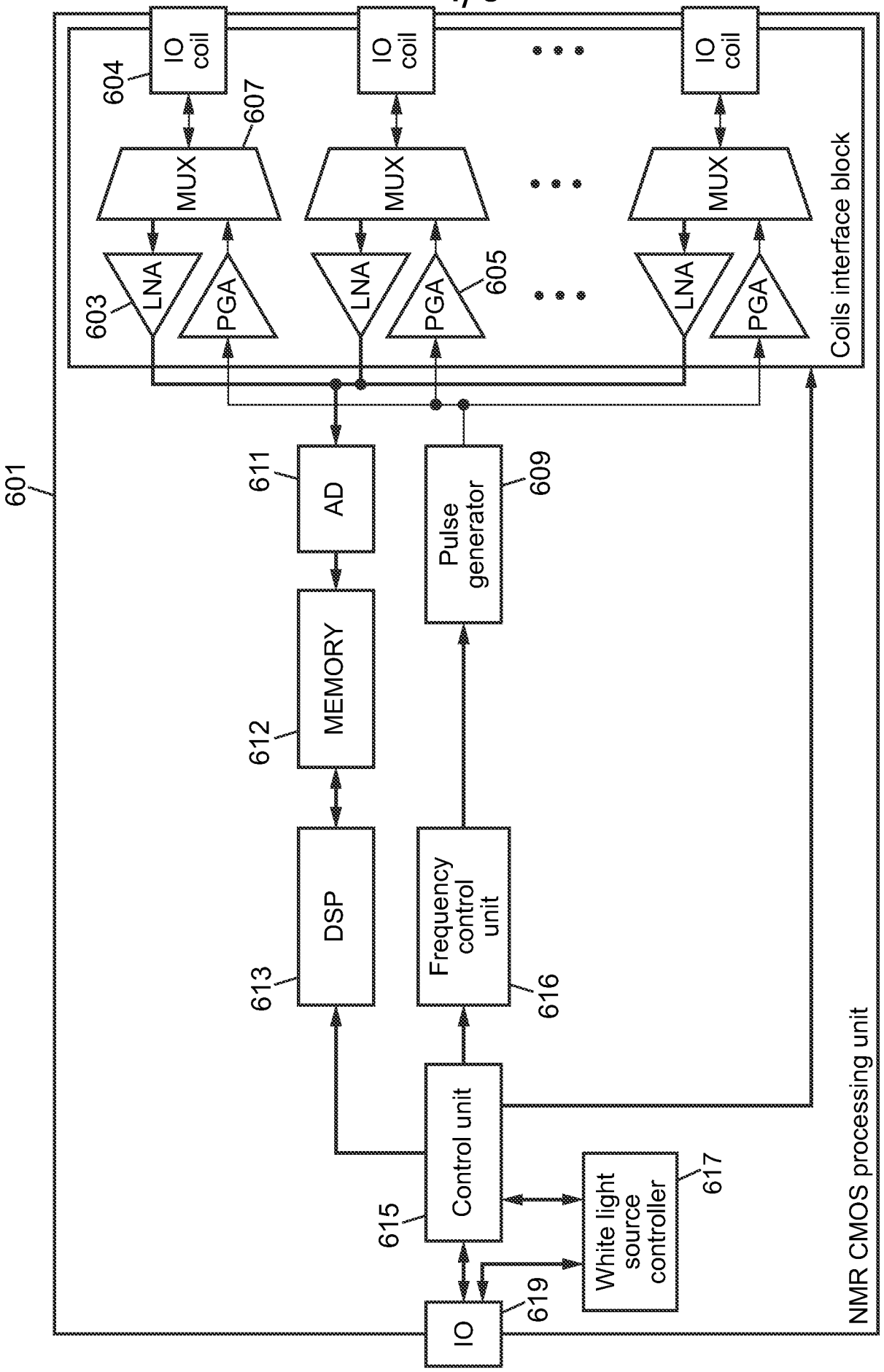
601
604
IO coil
607
MUX
603
LNA
PGA
605
Coils interface block
611
AD
609
Pulse generator
612
MEMORY
613
DSP
Frequency control unit
616
615
Control unit
617
White light source controller
619
IO
NMR CMOS processing unit

FIG. 6

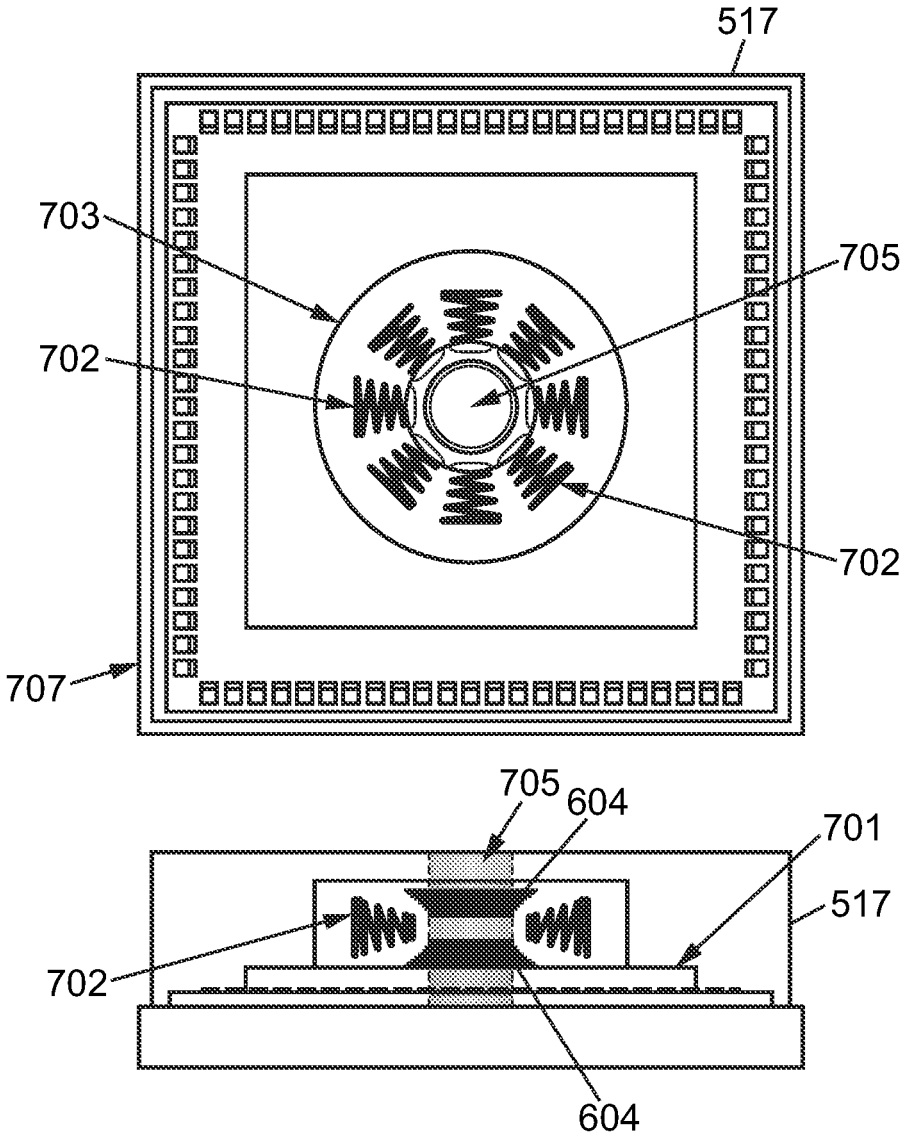

FIG. 7

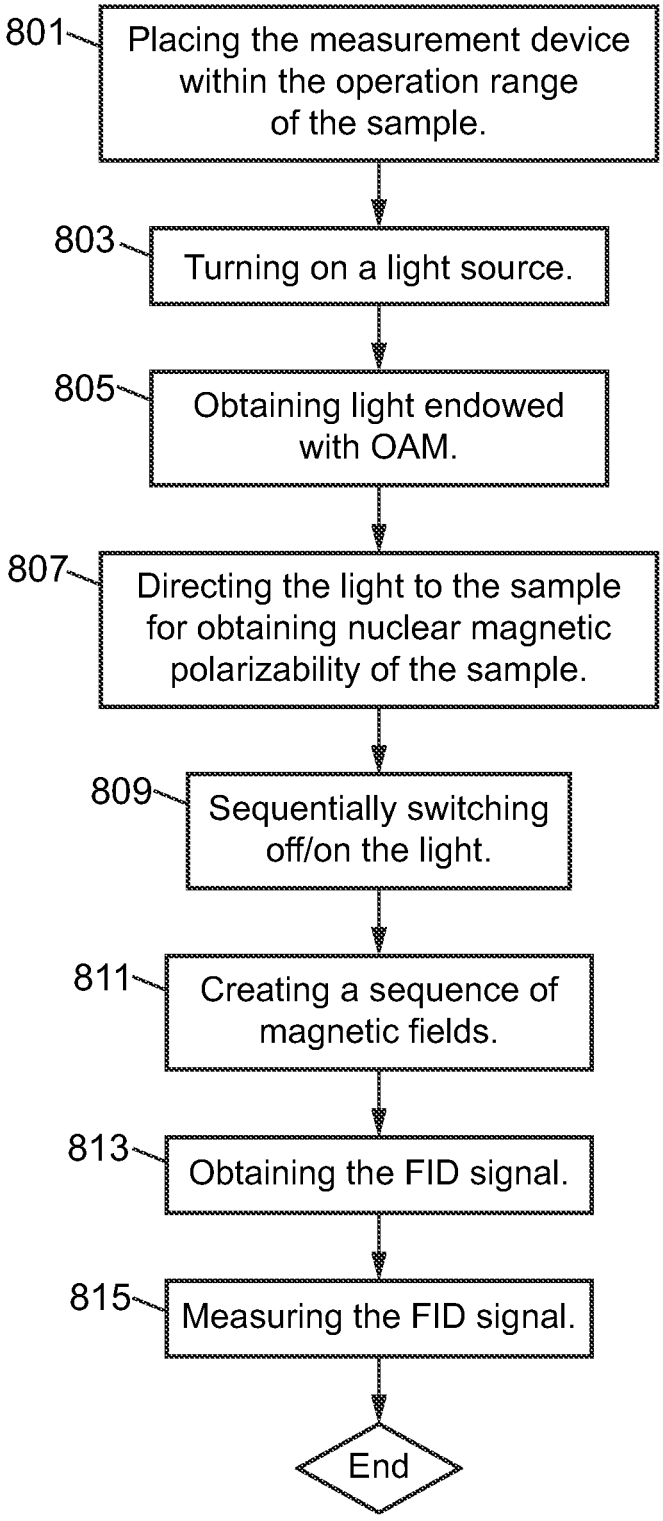
801
Placing the measurement device within the operation range of the sample.
803
Turning on a light source.
805
Obtaining light endowed with OAM.
807
Directing the light to the sample for obtaining nuclear magnetic polarizability of the sample.
809
Sequentially switching off/on the light.
811
Creating a sequence of magnetic fields.
813
Obtaining the FID signal.
815
Measuring the FID signal.
End

FIG. 8

INTERNATIONAL SEARCH REPORT

International application No
PCT/IB2009/050144

A. CLASSIFICATION OF SUBJECT MATTER
INV. G01N24/00 G01R33/46
ADD. G01R33/28 A61B5/00

According to International Patent Classification (IPC) or to both national classification and IPC

B. FIELDS SEARCHED

Minimum documentation searched (classification system followed by classification symbols)
G01N G01R

Documentation searched other than minimum documentation to the extent that such documents are included in the fields searched

Electronic data base consulted during the international search (name of data base and, where practical, search terms used)
EPO-Internal, WPI Data

C. DOCUMENTS CONSIDERED TO BE RELEVANT

Category*	Citation of document, with indication, where appropriate, of the relevant passages	Relevant to claim No.
A	WARREN W S ET AL: "Laser enhanced NMR spectroscopy, revisited" MOLECULAR PHYSICS, TAYLOR & FRANCIS, GB, vol. 93, no. 3, 20 February 1998 (1998-02-20), pages 371-375, XP009115496 ISSN: 0026-8976 the whole document	
A	BUCKINGHAM A D ET AL: "The effect of circularly polarized light on NMR spectra" MOLECULAR PHYSICS, TAYLOR & FRANCIS, GB, vol. 91, 1 August 1997 (1997-08-01), pages 805-814, XP009115500 ISSN: 0026-8976 the whole document	

-/--

[X] Further documents are listed in the continuation of Box C. [ ] See patent family annex.

* Special categories of cited documents :

"A" document defining the general state of the art which is not considered to be of particular relevance
"E" earlier document but published on or after the international filing date
"L" document which may throw doubts on priority claim(s) or which is cited to establish the publication date of another citation or other special reason (as specified)
"O" document referring to an oral disclosure, use, exhibition or other means
"P" document published prior to the international filing date but later than the priority date claimed
"T" later document published after the international filing date or priority date and not in conflict with the application but cited to understand the principle or theory underlying the invention
"X" document of particular relevance; the claimed invention cannot be considered novel or cannot be considered to involve an inventive step when the document is taken alone
"Y" document of particular relevance; the claimed invention cannot be considered to involve an inventive step when the document is combined with one or more other such documents, such combination being obvious to a person skilled in the art.
"&" document member of the same patent family

Date of the actual completion of the international search	Date of mailing of the international search report
28 April 2009	07/05/2009

Name and mailing address of the ISA/	Authorized officer
European Patent Office, P.B. 5818 Patentlaan 2 NL – 2280 HV Rijswijk Tel. (+31-70) 340-2040, Fax: (+31-70) 340-3016	Raguin, Guy

INTERNATIONAL SEARCH REPORT

International application No
PCT/IB2009/050144

C(Continuation). DOCUMENTS CONSIDERED TO BE RELEVANT

Category*	Citation of document, with indication, where appropriate, of the relevant passages	Relevant to claim No.
A	COURTIAL ET AL: "Gaussian beams with very high orbital angular momentum" OPTICS COMMUNICATIONS, NORTH-HOLLAND PUBLISHING CO. AMSTERDAM, NL, vol. 144, no. 4-6, 15 December 1997 (1997-12-15), pages 210-213, XP022575372 ISSN: 0030-4018 the whole document	
A	ALLEN L ET AL: "THE ORBITAL ANGULAR MOMENTUM OF LIGHT" PROGRESS IN OPTICS, XX, XX, vol. 39, 1 January 1999 (1999-01-01), pages 291-372, XP009115478 the whole document	

FURTHER INFORMATION CONTINUED FROM PCT/ISA/ 210

Continuation of Box II.2

Claims Nos.: -

1 Reference is made to the following documents:

D1: WARREN W S ET AL: "Laser enhanced NMR spectroscopy, revisited" MOLECULAR PHYSICS, TAYLOR & FRANCIS, vol. 93, no. 3, 20 February 1998 (1998-02-20), pages 371-375, XP009115496 ISSN: 0026-8976

D2: BUCKINGHAM A D ET AL: "The effect of circularly polarized light on NMR spectra" MOLECULAR PHYSICS, TAYLOR & FRANCIS, vol. 91, 1 August 1997 (1997-08-01), pages 805-814, XP009115500 ISSN: 0026-8976

D3: COURTIAL ET AL: "Gaussian beams with very high orbital angular momentum" OPTICS COMMUNICATIONS, vol. 144, no. 4-6, 15 December 1997 (1997-12-15), pages 210-213, XP022575372 ISSN: 0030-4018

2 The non-compliance with the substantive provisions of Art. 5 and 6 PCT (see section "Re Item VIII" of the WO-ISA) is to such an extent that no meaningful assessment of novelty, an inventive step and industrial applicability of claims 1-15 could be carried out at all (Art. 17(2) PCT).

3 In addition to the objections raised in section "Re Item VIII" of the WO-ISA, the following is noted.

3.A With regards to clarity (Art. 6 PCT), the terminology used in the application is often very confusing. In particular, it seems the term "polarization" should have been used instead of the term "polarizability", and, in a similar way, any reference to "aligning nuclei" or "magnetons" would appear to actually refer to "aligning nuclear spins of the molecules of the fluid" defined in claim 1. Without these two amendments, the application as a whole would appear to make no sense at all. However, it is unclear whether there is sufficient support for these amendments (Article 19(2) and 34(2)(b) PCT).

3.B With regards to Art. 5 PCT, It would appear that the subject-matter of the application relies on the possibility of directly hyperpolarizing nuclear spins of atoms within molecules of a fluid using light with orbital angular momentum without the use of any external static magnetic field. However, the theoretical part of the description appears to be entirely speculative in nature (see e.g. page 24, lines 19-28) and there is no common general knowledge of this kind available to the person skilled in the art to support this thesis. The application as a whole is silent with regards to e.g. which nuclei can be hyperpolarized by light with OAM, how to select the nuclei to be hyperpolarized, and what is the relation between the precession frequency of the hyperpolarized nuclear spins and the experimental parameters (light spectrum, OAM, ...).

Moreover, the one and only embodiment disclosed in the description fails to provide any experimental evidence that said desired technical effect is actually obtained, since no experimental data is presented. The description merely discloses the "acquisition of the magnetic FID of

a sample illuminated with light with spin and OAM" and the "FID coming from the not illuminated sample". In the absence of any disclosed FID and any analysis of said FIDs, it is however unclear what was actually measured and whether said FIDs actually result from the desired technical effect. It is noted for example that D1 and D2 (and references therein) disclose the controversy that existed for several years as to whether circularly polarized light could induce a detectable shift in NMR spectra due to the inverse Faraday effect (the magnetic field induced locally at the nuclei by the electromagnetic wave). After further analysis and experiments, it was agreed that no detectable shifts is possible and any shift that was detected resulted from thermal effects. In a similar way, if any actual FIDs were measured by the present embodiment, there is no sufficient evidence to attribute them to the desired technical effect, since a detailed analysis of other possible reasons has not been disclosed.

Therefore, it appears as though the successful performance of the invention is dependent on chance (PCT/GL/ISPE 4.13(a)), such that the application lacks sufficient disclosure.

3.C Moreover, it is noted that the subject-matter of all independent claims (claims 1, 9 and 10) would appear to lack novelty, should the objections under Art. 6 PCT raised in section "Re Item VIII" of the WO-ISA and in item 3.A above be ignored. More specifically, the wording of independent claims 1, 9 and 10, respectively, is so broad, that any documents disclosing nuclear magnetic resonance (NMR) spectroscopy, a computer program carrying instructions to implement NMR spectroscopy, and a NMR spectrometer, respectively, would be novelty destroying.

The applicant's attention is drawn to the fact that claims relating to inventions in respect of which no international search report has been established need not be the subject of an international preliminary examination (Rule 66.1(e) PCT). The applicant is advised that the EPO policy when acting as an International Preliminary Examining Authority is normally not to carry out a preliminary examination on matter which has not been searched. This is the case irrespective of whether or not the claims are amended following receipt of the search report or during any Chapter II procedure. If the application proceeds into the regional phase before the EPO, the applicant is reminded that a search may be carried out during examination before the EPO (see EPO Guideline C-VI, 8.2), should the problems which led to the Article 17(2)PCT declaration be overcome.

INTERNATIONAL SEARCH REPORT

International application No.
PCT/IB2009/050144

Box No. II Observations where certain claims were found unsearchable (Continuation of item 2 of first sheet)

This international search report has not been established in respect of certain claims under Article 17(2)(a) for the following reasons:

1. ☐ Claims Nos.:
because they relate to subject matter not required to be searched by this Authority, namely:

2. ☒ Claims Nos.:
because they relate to parts of the international application that do not comply with the prescribed requirements to such an extent that no meaningful international search can be carried out, specifically:

see FURTHER INFORMATION sheet PCT/ISA/210

3. ☐ Claims Nos.:
because they are dependent claims and are not drafted in accordance with the second and third sentences of Rule 6.4(a).

Box No. III Observations where unity of invention is lacking (Continuation of item 3 of first sheet)

This International Searching Authority found multiple inventions in this international application, as follows:

1. ☐ As all required additional search fees were timely paid by the applicant, this international search report covers allsearchable claims.

2. ☐ As all searchable claims could be searched without effort justifying an additional fees, this Authority did not invite payment of additional fees.

3. ☐ As only some of the required additional search fees were timely paid by the applicant, this international search reportcovers only those claims for which fees were paid, specifically claims Nos.:

4. ☐ No required additional search fees were timely paid by the applicant. Consequently, this international search report is restricted to the invention first mentioned in the claims; it is covered by claims Nos.:

Remark on Protest

☐ The additional search fees were accompanied by the applicant's protest and, where applicable, the payment of a protest fee.

☐ The additional search fees were accompanied by the applicant's protest but the applicable protest fee was not paid within the time limit specified in the invitation.

☐ No protest accompanied the payment of additional search fees.